

# A COMPLEX AND TRIPLEX FRAMEWORK FOR ENCODING THE RIEMANNIAN DUAL SPACE-TIME TOPOLOGY EQUIPPED WITH ORDER PARAMETER FIELDS

**N. O. Schmidt**

Department of Mathematics  
Boise State University  
1910 University Drive  
Boise, Idaho 83725, USA  
nathanschmidt@u.boisestate.edu

## **Abstract**

In this work, we forge a powerful, easy-to-visualize, flexible, consistent, and disciplined abstract vector framework for particle and astro physics that is compliant with the holographic principle. We demonstrate that the structural properties of the complex number and the sphere enable us to introduce and define the *triplex number*—an influential information structure that is similar to the 3D hyper-complex number by D. White and P. Nylander—which identifies a 3D analogue of (2D) complex space. Consequently, we engage the complex and triplex numbers as abstract vectors to systematically encode the state space of the Riemannian dual 3D *and* 4D space-time topologies, where space and time are dual and interconnected; we use the triplex numbers (with *triplex multiplication*) to extend 1D and 2D algebraic systems to 3D and 4D configurations. In doing so, we equip space-time with order parameter fields for topological deformations. Finally, to exemplify our motivation, we provide three example applications for this framework.

**Keywords:** Holographic principle; Holographic ring; Riemannian circle; Riemann surface; Space-time duality; Topology; Topological deformations; Order Parameters; Superfluids; Spontaneous Symmetry breaking; Generalized coordinates; Complex numbers; Triplex numbers; Triplex multiplication; Color confinement; Baryon wavefunction; Antisymmetry; Black holes; Quasi-normal modes; Computer graphics; Fractals; Mandelbulb.

## 1 Introduction

The term “information” is notorious for having *many* different forms and meanings [1]. *So in the limited context of this paper, what definition of information are we interested in?* Here, we ascertain that information is defined as: a sequence of symbols that can encode a message *and* any type of event that affects the state of a dynamical system. A complex number can be used to encode information—it is a number that can be put in the form

$$x = x_{\mathbb{R}} + x_{\mathbb{I}}, \tag{1}$$

where  $x_{\mathbb{R}}$  is the *real* component and  $x_{\mathbb{I}}$  is the *imaginary* component of the complex number  $x$  [2, 3]. Eq. (1) is important because it stores abstract information by extending the 1D number line to the 2D complex plane by using the horizontal axis for  $x_{\mathbb{R}}$  and the vertical axis for  $x_{\mathbb{I}}$ . Hence,  $x$  can be identified with the point  $(x_{\mathbb{R}}, x_{\mathbb{I}})$  in a 2D Cartesian coordinate system called the complex plane  $X$ , such that  $x \in X$  [2, 3]. Thus,  $x$  is a scalar that simultaneously encodes the *magnitude* and *direction* components of a vector [2, 3]. If  $x_{\mathbb{R}} = 0$ , then  $x$  is said to be purely imaginary, whereas if  $x_{\mathbb{I}} = 0$ , then  $x$  is said to be purely real [2, 3]. In this way, eq. (1) comprises the familiar real numbers and therefore equips us with the means to attack problems, encode states in state space, and deal with patterns that cannot be realized by real numbers alone.

Eq. (1) provides a wide variety of applications in science and engineering. For example, in quantum physics the wavefunction—with values typically stored in the form of eq. (1)—characterizes the quantum state of a particle and its behavior; the Schrödinger equation designates how the wavefunction evolves in space over time [4]. In computer and electrical engineering, eq. (1) can be applied to represent sinusoidal oscillating voltage and current in circuit analysis and design [5]. In fractal geometry, the language of chaos theory [6], information encoded using eq. (1) can represent input and output values of iterated functions that generate fractals such as B. Mandelbrot’s set [7]—self-similar patterns that are *abundant* in nature [8, 9]. Indeed, the concept put forth by eq. (1) is intrinsic to encoding the abstract features of G. ’t Hooft’s and L. Susskind’s “holographic universe” [10, 11, 12] by applying the state space  $X$ .

Another familiar mathematical construct that is fundamental to nature is the sphere. For example, spherically-symmetric structures are often used as the mathematical underpinnings for understanding gravity [13, 14, 15, 16], black holes and space-time [17, 18, 19], stars [20, 21, 22], nuclear mass [23, 24, 25], and more. Now in terms of spontaneous symmetry breaking, imagine that the surface of a spherically-symmetric structure can be equipped with abstract vectors or order parameters [26, 27] to encode topological deformations [28, 29, 30, 31] as in the analytic color-anticolor confinement and baryon-antibaryon duality proof of [32]. In this context, it is useful to imagine that the “base case”, a circle (1-sphere)  $T$ , can be isometrically embedded in  $X$ , such that  $T \subset X$ , where  $T$  can be topologically deformed to represent any conceivable elliptical case to encode, for example, an orbital system of massive bodies—see Figure 1. Similarly, if we imagine the case of  $T$  being a 2-sphere that is isometrically embedded in the 3D real manifold  $Y$ , such that  $X \subset Y$  and  $T \subset Y$ , then we see that  $T$  can be topologically deformed to represent any conceivable spheroid case to encode, for example,

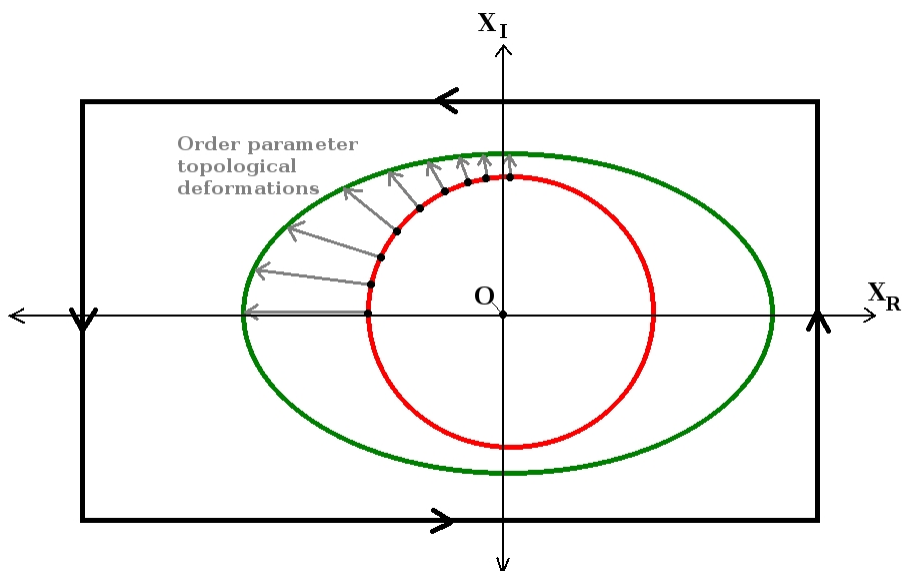


Fig. 1: A circle can be transformed into a non-circular ellipse by equipping it with order parameters for topological deformations.

a planet in our solar system. Furthermore, if the topological deformation order parameters along the 1-sphere or 2-sphere are used to encode fractional statistics as in [32], then encoding a fractal state space [7] becomes relatively straightforward. In this work, we will follow [32] and demonstrate that a space-time topology equipped with an embedded 1-sphere or 2-sphere and order parameters is an essential *non-linear* component of the “holographic principle” that is axiomatic to quantum gravity and string theories [10, 11, 12].

In this paper, we combine eq. (1) with spherical concepts to establish a mathematical definition of *triplex numbers* with *triplex multiplication* that simplifies the 3D hyper-complex number and its operators by D. White and P. Nylander [33, 34, 35]. We engage the complex and triplex numbers as abstract scalars *and* vectors to frame the position and order parameter states of a spherically-symmetric system that can be directly applied as information structures to encode chaotic systems—dynamical systems that are highly sensitive to initial conditions [6, 7, 36, 37]. In general, this new and developing framework focuses on improving the Riemannian dual (“fractional quantum Hall superfluidic”) space-time topology and representational capability for the analytic confinement, duality, and antisymmetry proof of [32] that is consistent with holographic models [10, 11, 12].

In Section 2, we fashion the *Riemannian dual 3D space-time*, where the time dimension is a topological circle  $T$  that is isometrically embedded in a Riemann surface  $X$ , such that  $T$  is simultaneously dual to two spatial sub-surfaces—an improvement to [32]. First, we upgrade the dual 3D space-time topology of [32] by exercising the complex numbers as “2D position vectors” to engineer  $X$ , namely the *2D position-point state space* (2D-PPSS), with complex locations in the form of eq. (1), namely *2D position-point states* (2D-PPS), that are identified by *2D generalized Riemannian-coordinates*. Next, we refine the simultaneous

superfluidic symmetry breaking representation of [32] by additionally using the complex numbers as “2D order parameters” to install, at each 2D-PPS, a *2D order parameter state space* (2D-OPSS) with a spontaneous *2D order parameter state* (2D-OPS).

In Section 3, we devise the *Riemannian dual 4D space-time* by embedding the 2D-PPSS  $X$  in a 3D manifold  $Y$ , where the time dimension  $T$  becomes a topological Riemannian circle (2-sphere) [38] that is isometrically embedded in  $Y$ , such that  $T$  is simultaneously dual to two spatial 3-branes—an additional improvement to [32]. First, we upgrade the dual 4D space-time topology of [32] by defining the triplex numbers and applying them as “3D position vectors” to engineer  $Y$ , namely the *3D position-point state space* (3D-PPSS), with triplex locations, namely *3D position-point states* (3D-PPS), that are identified by *3D generalized Riemannian-coordinates*; this is paramount because it enables us to extend the lower dimensional algebraic systems to 4D space-time. Next, we enhance the simultaneous superfluidic symmetry breaking representation of [32] by additionally using the triplex numbers as “3D order parameters” to install, at each 3D-PPS, a *3D order parameter state space* (3D-OPSS) with a spontaneous *3D order parameter state* (3D-OPS).

In Section 4, we bestow three distinct and introductory examples that apply the triplex framework of Section 3 to particle physics, astro physics, and fractal geometry. First, we begin to merge our scenario with the “*White-Nylander mythical beast*” by identifying the triplex multiplication for computer graphics and simulating 3D fractals [33, 34, 35]. Second, we upgrade the fractional quantum number representations of the baryon wavefunction and antisymmetric tensor in [32] from 2D-OPSs to 3D-OPSs. And third, we supply an encoding methodology for the Schwarzschild black hole (SBH) quasi-normal modes of [39, 40, 41, 42, 43, 44].

Finally, in Section 5, we conclude with a brief recapitulation and discussion of the paper. Here, we highlight the importance of this framework and suggest future modes of exploration.

## 2 The complex framework for Riemannian dual 3D space-time

Here, starting with eq. (1), we assemble the complex information structures and encoding methodology for our 3D space-time, where the time dimension is the topological circle  $T$  that delineates dual spatial sub-surfaces on  $X$ ;  $T$  is simultaneously dual to two spatial distance scales as in [32]. This topological foundation is equipped with a 2D-PPSS and 2D-OPSS—see Table 1 for an introduction.

### 2.1 The 2D position-point state space

Here, we construct the 2D-PPSS and 2D generalized Riemannian-coordinates for the dual 3D space-time.

From [32], let the Riemann surface  $X$  be a 2D-PPSS. We define a 2D-PPS  $\vec{x} \in X$  in the 2D-PPSS  $X$  as a 2-number, complex number, complex scalar, and complex vector that encodes a location on (or within)  $X$ , where we refine eq. (1) as

$$\vec{x} \equiv \vec{x}_{\mathbb{R}} + \vec{x}_{\mathbb{I}}, \quad \forall \vec{x} \in X. \quad (2)$$

Simply put,  $\vec{x}$  is a state within the state space  $X$ .  $\vec{x}$  is expressed in terms of *2D Riemannian-coordinates*, which are well-defined generalized coordinates that *synchronize* 1D Complex-

Table 1: A summary of the complex framework with the 2D-PPSS (locations) and 2D-OPSS (features) for dual 3D space-time.

Complex Location Name	Complex Location Value
1D-PPS Complex-coordinate	$(\vec{x})$
2D-PPS Cartesian-coordinate	$(\vec{x}_{\mathbb{R}}, \vec{x}_{\mathbb{I}})$
2D-PPS Polar-coordinate	$( \vec{x} , \langle \vec{x} \rangle)$
2D-PPS Riemannian-coordinate	$(\vec{x}) = (\vec{x}_{\mathbb{R}}, \vec{x}_{\mathbb{I}}) = ( \vec{x} , \langle \vec{x} \rangle)$
Complex Feature Name	Complex Feature Value
1D-OPS Complex-vector	$(\vec{\psi}(\vec{x}))$
2D-OPS Cartesian-vector	$(\vec{\psi}(\vec{x})_{\mathbb{R}}, \vec{\psi}(\vec{x})_{\mathbb{I}})$
2D-OPS Polar-vector	$( \vec{\psi}(\vec{x}) , \langle \vec{\psi}(\vec{x}) \rangle)$
2D-OPS Riemannian-vector	$(\vec{\psi}(\vec{x})) = (\vec{\psi}(\vec{x})_{\mathbb{R}}, \vec{\psi}(\vec{x})_{\mathbb{I}}) = ( \vec{\psi}(\vec{x}) , \langle \vec{\psi}(\vec{x}) \rangle)$

coordinates, 2D Polar-coordinates, and 2D Cartesian-coordinates in a single *interconnected* “Complex-Polar-Cartesian-coordinate system”, namely the *2D Riemannian-coordinate system*: we augment eq. (2) with its corresponding *2D-PPS Riemannian-coordinate*, which identifies a

- *1D-PPS Complex-coordinate* with component

1. *complex-PPS*, namely  $\vec{x} \in X$ ,

for

$$\vec{x} \equiv (\vec{x}) = (\vec{x}_{\mathbb{R}} + \vec{x}_{\mathbb{I}}), \quad \forall \vec{x} \in X; \quad (3)$$

- *2D-PPS Polar-coordinate* (or “2D-PPS Circular-coordinate”) with components

1. *amplitude-PPS* (“radius” or “modulus”, previously “magnitude”), namely  $|\vec{x}| \in [0, \infty_{\mathbb{R}}]$ , and
2. *phase-PPS* (“azimuth”, previously “direction”), namely  $\langle \vec{x} \rangle \in [0, 2\pi]$ ,

for

$$\vec{x} \equiv (|\vec{x}|, \langle \vec{x} \rangle), \quad \forall \vec{x} \in X; \quad (4)$$

and

- *2D-PPS Cartesian-coordinate* (or “2D-PPS Box-coordinate”) with components

1. *real-PPS* (“ $\mathbb{R}$ ” or “ $x$ ”), namely  $\vec{x}_{\mathbb{R}} \in [-\infty_{\mathbb{R}}, \infty_{\mathbb{R}}]$ , and
2. *imaginary-PPS* (“ $\mathbb{I}$ ” or “ $y$ ”), namely  $\vec{x}_{\mathbb{I}} \in [-\infty_{\mathbb{I}}, \infty_{\mathbb{I}}]$ ,

for

$$\vec{x} \equiv (\vec{x}_{\mathbb{R}}, \vec{x}_{\mathbb{I}}), \quad \forall \vec{x} \in X, \quad (5)$$

with the synchronizing Pythagorean and trigonometric interconnection constraints

$$\begin{aligned}
 |\vec{x}| &\equiv \sqrt{\vec{x}_{\mathbb{R}}^2 + \vec{x}_{\mathbb{I}}^2} \\
 \vec{x}_{\mathbb{R}} &\equiv |\vec{x}| \cos\langle\vec{x}\rangle \\
 \vec{x}_{\mathbb{I}} &\equiv |\vec{x}| \sin\langle\vec{x}\rangle
 \end{aligned} \tag{6}$$

that generalize eqs. (7–9) in [32] to define the 2D-PPS Riemannian-coordinate

$$\vec{x} \equiv (\vec{x}) = (|\vec{x}|, \langle\vec{x}\rangle) = (\vec{x}_{\mathbb{R}}, \vec{x}_{\mathbb{I}}), \quad \forall \vec{x} \in X, \tag{7}$$

that generalizes eq. (10) in [32] and can be arranged into the row-vectors

$$\vec{x} \equiv [|\vec{x}|, \langle\vec{x}\rangle] = [\vec{x}_{\mathbb{R}}, \vec{x}_{\mathbb{I}}] \tag{8}$$

and the column-vectors

$$\vec{x} \equiv \begin{bmatrix} |\vec{x}| \\ \langle\vec{x}\rangle \end{bmatrix} = \begin{bmatrix} \vec{x}_{\mathbb{R}} \\ \vec{x}_{\mathbb{I}} \end{bmatrix} \tag{9}$$

for matrix notation. Subsequently, we use eq. (7) to define the reference frame  $O \in X$  as the localized *origin-point* of  $X$  as

$$O \equiv (0) = (0, 0) = (0, 0). \tag{10}$$

See Figure 2 for a straightforward depiction of this construction.

*So what notation do we use to represent multiple 2D-PPSs in  $X$ ?* Well, for  $n$  2D-PPSs we can use numerical characters as additional subscripts to simply extend the notation of eq. (7). Thus, using eq. (7) we may express the ordered set  $\{\vec{x}_1, \vec{x}_2, \dots, \vec{x}_n\} \subset X$  for  $n$  distinct 2D-PPSs with the corresponding 2D Riemannian-coordinates

$$\begin{aligned}
 1 : \vec{x}_1 &= (\vec{x}_1) = (|\vec{x}_1|, \langle\vec{x}_1\rangle) = (\vec{x}_{1\mathbb{R}}, \vec{x}_{1\mathbb{I}}) \\
 2 : \vec{x}_2 &= (\vec{x}_2) = (|\vec{x}_2|, \langle\vec{x}_2\rangle) = (\vec{x}_{2\mathbb{R}}, \vec{x}_{2\mathbb{I}}) \\
 &\dots \\
 n : \vec{x}_n &= (\vec{x}_n) = (|\vec{x}_n|, \langle\vec{x}_n\rangle) = (\vec{x}_{n\mathbb{R}}, \vec{x}_{n\mathbb{I}}).
 \end{aligned} \tag{11}$$

*So we've defined  $X$  as the 2D-PPSS, but how do we incorporate the time dimension to construct a 3D space-time, where space and time are dual and interconnected?* To answer this, we define the topological circle  $T \subset X$  as the *time zone*, *temporal sub-surface*, and “Inopin Holographic Ring” of “amplitude-radius” or “amplitude-modulus”  $\epsilon$  that is isometrically embedded in  $X$  [32];  $T$  is a closed time-like curve [45] and simple contour of topological surface 2D-PPSs. Following [32], we use “2D zone trichotomy” to simultaneously define the *micro space zone*  $X_-$  and the *macro space zone*  $X_+$ ;  $T$  is dual to *both*  $X_-$  and  $X_+$  *spatial sub-surfaces* as in [32]. So from eqs. (12–14) in [32], we know that  $\forall \vec{x} \in X$  precisely one of the following conditions must be satisfied

$$\begin{aligned}
 |\vec{x}| < \epsilon &\Leftrightarrow \vec{x} \in X_- \subset X \\
 |\vec{x}| = \epsilon &\Leftrightarrow \vec{x} \in T \subset X \\
 |\vec{x}| > \epsilon &\Leftrightarrow \vec{x} \in X_+ \subset X,
 \end{aligned} \tag{12}$$

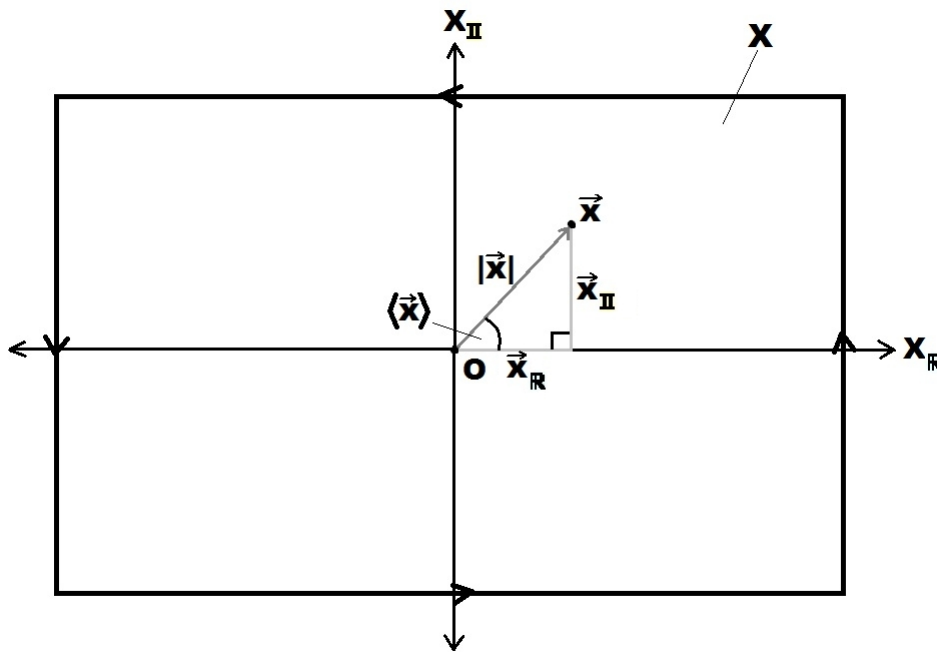


Fig. 2: The Riemann (space-time) surface and 2D-PPSS  $X$  contains a “real-axis” and an “imaginary-axis” and is equipped with a generalized 2D Riemannian-coordinate system that synchronizes 1D Complex-coordinates, 2D Polar-coordinates, and 2D Cartesian-coordinates. In this depiction,  $O \in X$  is  $X$ ’s distinct and localized origin-point and reference frame, while  $\vec{x} \in X$  is a 2D-PPS, which are both states on (or within)  $X$ . This simple and intuitive construction encodes locations on  $X$ .

where clearly  $X_- \cap T = T \cap X_+ = X_- \cap X_+ = \emptyset$  and  $X_- \cup T \cup X_+ = X$ . Hence, from eq. (15) in [32]  $T$  is the multiplicative group of all non-zero 2D-PPSs, such that

$$T \equiv \{\vec{x} \in X : |\vec{x}| = \epsilon\}, \tag{13}$$

and from eqs. (16–17) in [32] the micro and macro spatial sub-surface zones are defined as

$$\begin{aligned} X_- &\equiv \{\vec{x} \in X : |\vec{x}| < \epsilon\} \\ X_+ &\equiv \{\vec{x} \in X : |\vec{x}| > \epsilon\}. \end{aligned} \tag{14}$$

So clearly

$$\epsilon \equiv |\vec{x}| = \sqrt{x_{\mathbb{R}}^2 + \vec{x}_{\mathbb{I}}^2}, \quad \forall \vec{x} \in T, \tag{15}$$

$$|\vec{x}| = \sqrt{\vec{x}_{\mathbb{R}}^2 + \vec{x}_{\mathbb{I}}^2}, \quad \forall \vec{x} \in X, \tag{16}$$

which generalize eqs. (18–19) in [32]. So  $T$  is isometrically embedded in  $X$  with the one-to-one holographic mappings  $g : T \hookrightarrow X$  and  $g : T \rightarrow X_- \cup X_+$  with dual simultaneous bijections

$$\begin{aligned} {}^{2D}g_{time} : X_- &\leftrightarrow T \hookrightarrow X_+ \\ {}^{2D}g_{space} : X_- &\hookrightarrow T \leftrightarrow X_+ \end{aligned} \tag{17}$$

for our *dual* 3D space-time that generalize eqs. (20–21) in [32]. Thus, the temporal sub-surface  $T$  serves as a *common 1D surface boundary* between the dual interconnected  $X_-$  and  $X_+$  spatial sub-surfaces as in [32]; this is consistent with the holographic principle [10, 11, 12].

At this point, we've successfully defined the Riemannian dual 3D space-time topology; this is a direct upgrade to the topological framework of [32]. In Section 3.1, we will explain how to extend  $X$  from 3D to 4D space-time.

## 2.2 The 2D order parameter state space

$\forall \vec{x} \in X$ , we may assign one or more *2D-OPSS layers*, where each layer corresponds to a distinct 2D-OPSS with a spontaneously selected 2D-OPS. Following [32], these quantifiable features may represent fractional statistics and are expressed using a notation that is virtually identical to the 2D-PPS (and 2D-PPSS) eqs. (3–9) from the previous section. To illustrate the base case, we opt to assign *one* generic 2D-OPS layer to  $X$  to encode one type of feature. Hence, at the 2D-PPS  $\vec{x} \in X$ , we have the single generic 2D-OPS  $\vec{\psi}(\vec{x})$  in the 2D-OPSS  $\Phi(\vec{x})$ , where  $\vec{\psi}(\vec{x}) \in \Phi(\vec{x})$ , such that  $\Phi(\vec{x})$  is the continuous and infinite set of 2D-OPSs (with cardinality  $|\Phi(\vec{x})| = \infty$ ) that is localized at  $\vec{x} \in X$ . Therefore, to generalize eq. (24) in [32] we define

$$\vec{\psi}(\vec{x}) \equiv \vec{\psi}(\vec{x})_{\mathbb{R}} + \vec{\psi}(\vec{x})_{\mathbb{I}}, \quad \forall \vec{x} \in X, \quad \forall \vec{\psi}(\vec{x}) \in \Phi(\vec{x}), \tag{18}$$

which is expressed in the *2D-OPS Riemannian-vector* notation that synchronizes and simultaneously references three vector systems. Simply put,  $\vec{\psi}(\vec{x})$  is a state in the state space

$\Phi(\vec{x})$ . Thus, to augment eq. (18) we use the 1D-PPS Complex-coordinate notation of eq. (3) to construct the *1D-OPS Complex-vector*

$$\vec{\psi}(\vec{x}) \equiv (\vec{\psi}(\vec{x})) = (\vec{\psi}(\vec{x})_{\mathbb{R}} + \vec{\psi}(\vec{x})_{\mathbb{I}}), \quad \forall \vec{\psi}(\vec{x}) \in \Phi(\vec{x}). \quad (19)$$

Similarly, we use the 2D-PPS Polar-coordinate notation of eq. (4) to construct the *2D-OPS Polar-vector* (or “2D-OPS Circular-vector”)

$$\vec{\psi}(\vec{x}) \equiv (|\vec{\psi}(\vec{x})|, \langle \vec{\psi}(\vec{x}) \rangle), \quad \forall \vec{\psi}(\vec{x}) \in \Phi(\vec{x}), \quad (20)$$

with components *amplitude-OPS*  $|\vec{\psi}(\vec{x})| \in [0, \infty_{\mathbb{R}}]$  and *phase-OPS*  $\langle \vec{\psi}(\vec{x}) \rangle \in [0, 2\pi]$ , respectively. Subsequently, we use the 2D-PPS Cartesian-coordinate notation of eq. (5) to construct the *2D-OPS Cartesian-vector* (or “2D-OPS Box-vector”)

$$\vec{\psi}(\vec{x}) \equiv (\vec{\psi}(\vec{x})_{\mathbb{R}}, \vec{\psi}(\vec{x})_{\mathbb{I}}), \quad \forall \vec{\psi}(\vec{x}) \in \Phi(\vec{x}), \quad (21)$$

with components *real-OPS*  $\vec{\psi}(\vec{x})_{\mathbb{R}} \in [-\infty_{\mathbb{R}}, \infty_{\mathbb{R}}]$  and *imaginary-OPS*  $\vec{\psi}(\vec{x})_{\mathbb{I}} \in [-\infty_{\mathbb{I}}, \infty_{\mathbb{I}}]$ , respectively. Eqs. (19–21) satisfy the synchronizing Pythagorean and trigonometric inter-connection constraints

$$\begin{aligned} |\vec{\psi}(\vec{x})| &\equiv \sqrt{\vec{\psi}^2(\vec{x})_{\mathbb{R}} + \vec{\psi}^2(\vec{x})_{\mathbb{I}}} \\ \vec{\psi}(\vec{x})_{\mathbb{R}} &\equiv |\vec{\psi}(\vec{x})| \cos \langle \vec{\psi}(\vec{x}) \rangle \\ \vec{\psi}(\vec{x})_{\mathbb{I}} &\equiv |\vec{\psi}(\vec{x})| \sin \langle \vec{\psi}(\vec{x}) \rangle \end{aligned} \quad (22)$$

to define the 2D-OPS Riemannian-vector

$$\vec{\psi}(\vec{x}) \equiv (\vec{\psi}(\vec{x})) = (|\vec{\psi}(\vec{x})|, \langle \vec{\psi}(\vec{x}) \rangle) = (\vec{\psi}(\vec{x})_{\mathbb{R}}, \vec{\psi}(\vec{x})_{\mathbb{I}}), \quad \forall \vec{\psi}(\vec{x}) \in \Phi(\vec{x}), \quad (23)$$

which can be arranged into the row-vectors

$$\vec{\psi}(\vec{x}) \equiv [|\vec{\psi}(\vec{x})|, \langle \vec{\psi}(\vec{x}) \rangle] = [\vec{\psi}(\vec{x})_{\mathbb{R}}, \vec{\psi}(\vec{x})_{\mathbb{I}}] \quad (24)$$

and the column-vectors

$$\vec{\psi}(\vec{x}) \equiv \begin{bmatrix} |\vec{\psi}(\vec{x})| \\ \langle \vec{\psi}(\vec{x}) \rangle \end{bmatrix} = \begin{bmatrix} \vec{\psi}(\vec{x})_{\mathbb{R}} \\ \vec{\psi}(\vec{x})_{\mathbb{I}} \end{bmatrix} \quad (25)$$

for matrix notation.

Next, we define the various types of 2D-OPSs that give us extreme flexibility for encoding features such as topological deformations and wavefunction components of [32]. For this, we can employ 2D-OPSs to represent the *specific* quantum number deformation states of [32] or to represent more *general* deformation states that may be applied to other physics models. To encode a dynamical system state with our complex framework, we are free to use both categories separately or in conjunction with each other—our choice depends entirely on the representational scope of the problem domain and its inherent complexity. For example,

if we wish to specifically encode the quantum number states of magnetic charge, electric charge, color charge, isospin, orbital angular momentum, spin angular momentum, and total angular momentum for the baryon topological deformations, wavefunctions, and tensors in [32], then we can apply eq. (23)  $\forall \vec{x} \text{ in } X$  to define the respective specific 2D-OPSS (in short form) as

$$\begin{aligned}
 \vec{\psi}_B(\vec{x}) &\equiv (\vec{\psi}_B(\vec{x})), \quad \forall \vec{\psi}_B(\vec{x}) \in \Phi_B(\vec{x}) \\
 \vec{\psi}_E(\vec{x}) &\equiv (\vec{\psi}_E(\vec{x})), \quad \forall \vec{\psi}_E(\vec{x}) \in \Phi_E(\vec{x}) \\
 \vec{\psi}_C(\vec{x}) &\equiv (\vec{\psi}_C(\vec{x})), \quad \forall \vec{\psi}_C(\vec{x}) \in \Phi_C(\vec{x}) \\
 \vec{\psi}_I(\vec{x}) &\equiv (\vec{\psi}_I(\vec{x})), \quad \forall \vec{\psi}_I(\vec{x}) \in \Phi_I(\vec{x}) \\
 \vec{\psi}_L(\vec{x}) &\equiv (\vec{\psi}_L(\vec{x})), \quad \forall \vec{\psi}_L(\vec{x}) \in \Phi_L(\vec{x}) \\
 \vec{\psi}_S(\vec{x}) &\equiv (\vec{\psi}_S(\vec{x})), \quad \forall \vec{\psi}_S(\vec{x}) \in \Phi_S(\vec{x}) \\
 \vec{\psi}_J(\vec{x}) &\equiv (\vec{\psi}_J(\vec{x})), \quad \forall \vec{\psi}_J(\vec{x}) \in \Phi_J(\vec{x})
 \end{aligned} \tag{26}$$

Moreover, if we wish to encode topological deformation states without a specific reference to quantum numbers, then we can similarly apply eq. (23) to define the general and “generic” 2D-OPSS as

$$\vec{\psi}_{\rightarrow}(\vec{x}_1) \equiv (\vec{\psi}_{\rightarrow}(\vec{x}_1)), \quad \forall \vec{\psi}_{\rightarrow}(\vec{x}_1) \in \Phi_{\rightarrow}(\vec{x}_1), \quad \forall \vec{x}_1 \in X, \tag{27}$$

such that

$$\vec{x}_2 \equiv \vec{x}_1 + \vec{\psi}_{\rightarrow}(\vec{x}_1) \tag{28}$$

is the *effective 2D-PPS*  $\vec{x}_2 \in X$  that is identified by the deformation of  $\vec{\psi}_{\rightarrow}(\vec{x}_1)$  at  $\vec{x}_1$ . See Table 2 for a list of possible 2D-OPSS candidates that we may (or may not) opt to use in the dual 3D space-time.

Table 2: A list of possible 2D-OPSS candidates designed to encode topological deformation and wavefunction states in the dual 3D space-time.

Name	Symbol	2D Order Parameter State	Application
Magnetic Charge	$B$	$\vec{\psi}_B(\vec{x}) \equiv \vec{\psi}_B(\vec{x})_{\mathbb{R}} + \vec{\psi}_B(\vec{x})_{\mathbb{I}}$	Specific
Electric Charge	$E$	$\vec{\psi}_E(\vec{x}) \equiv \vec{\psi}_E(\vec{x})_{\mathbb{R}} + \vec{\psi}_E(\vec{x})_{\mathbb{I}}$	Specific
Color Charge	$C$	$\vec{\psi}_C(\vec{x}) \equiv \vec{\psi}_C(\vec{x})_{\mathbb{R}} + \vec{\psi}_C(\vec{x})_{\mathbb{I}}$	Specific
Isospin	$I$	$\vec{\psi}_I(\vec{x}) \equiv \vec{\psi}_I(\vec{x})_{\mathbb{R}} + \vec{\psi}_I(\vec{x})_{\mathbb{I}}$	Specific
Orbital Angular Momentum	$L$	$\vec{\psi}_L(\vec{x}) \equiv \vec{\psi}_L(\vec{x})_{\mathbb{R}} + \vec{\psi}_L(\vec{x})_{\mathbb{I}}$	Specific
Spin Angular Momentum	$S$	$\vec{\psi}_S(\vec{x}) \equiv \vec{\psi}_S(\vec{x})_{\mathbb{R}} + \vec{\psi}_S(\vec{x})_{\mathbb{I}}$	Specific
Total Angular Momentum	$J$	$\vec{\psi}_J(\vec{x}) \equiv \vec{\psi}_J(\vec{x})_{\mathbb{R}} + \vec{\psi}_J(\vec{x})_{\mathbb{I}}$	Specific
“Generic” Deformation	$\rightarrow$	$\vec{\psi}_{\rightarrow}(\vec{x}) \equiv \vec{\psi}_{\rightarrow}(\vec{x})_{\mathbb{R}} + \vec{\psi}_{\rightarrow}(\vec{x})_{\mathbb{I}}$	General

At this point, we’ve assembled the complex information structures and encoding methodology for our dual 3D space-time, where each 2D-PPS in the 2D-PPSS is equipped with a localized 2D-OPSS—recall Table 1. This is a direct refinement to the spontaneous symmetry breaking framework of [32]. Now, we are ready to incorporate an additional degree of freedom into our framework.

### 3 The triplex framework for Riemannian dual 4D space-time

Here, starting with the complex framework definitions of Section 2, we assemble the triplex information structures and encoding methodology for our 4D space-time, where the time dimension is the topological Riemannian circle  $T$  that delineates dual spatial 3-branes in  $Y$ ;  $T$  is simultaneously dual to two distance scales as in [32]. This topological foundation is equipped with a 3D-PPSS and 3D-OPSS—see Table 3 for an introduction.

Table 3: A summary of the triplex framework with the 3D-PPSS (locations) and 3D-OPSS (features) for dual 4D space-time.

<b>Triplex Location Name</b>	<b>Triplex Location Value</b>
1D-PPS Triplex-coordinate	$(\vec{y})$
3D-PPS Cartesian-coordinate	$(\vec{y}_{\mathbb{R}}, \vec{y}_{\mathbb{I}}, \vec{y}_Z)$
3D-PPS Polar-coordinate	$( \vec{y} , \langle \vec{y} \rangle, [\vec{y}])$
3D-PPS Riemannian-coordinate	$(\vec{y}) = (\vec{y}_{\mathbb{R}}, \vec{y}_{\mathbb{I}}, \vec{y}_Z) = ( \vec{y} , \langle \vec{y} \rangle, [\vec{y}])$
<b>Triplex Feature Name</b>	<b>Triplex Feature Value</b>
1D-OPS Triplex-vector	$(\vec{\psi}(\vec{y}))$
3D-OPS Cartesian-vector	$(\vec{\psi}(\vec{y})_{\mathbb{R}}, \vec{\psi}(\vec{y})_{\mathbb{I}}, \vec{\psi}(\vec{y})_Z)$
3D-OPS Polar-vector	$( \vec{\psi}(\vec{y}) , \langle \vec{\psi}(\vec{y}) \rangle, [\vec{\psi}(\vec{y})])$
3D-OPS Riemannian-vector	$(\vec{\psi}(\vec{y})) = (\vec{\psi}(\vec{y})_{\mathbb{R}}, \vec{\psi}(\vec{y})_{\mathbb{I}}, \vec{\psi}(\vec{y})_Z) = ( \vec{\psi}(\vec{y}) , \langle \vec{\psi}(\vec{y}) \rangle, [\vec{\psi}(\vec{y})])$

#### 3.1 The 3D position-point state space

Here, we assemble the 3D-PPSS and 3D generalized Riemannian-coordinates for the dual 4D space-time.

*So how can we extend  $X$  from 3D to 4D space-time?* Well first, we know that  $X$ , a Riemann surface and 2D-PPSS, can be thought of as a “deformed version” of the complex plane as in [32], and furthermore, we know that a Riemann surface can be expressed in terms of a function [46]. So for this topological application  $X$  must be deformed within, and be contained within, a higher dimensional information structure equipped with an additional degree of freedom. This is logical because Riemann surfaces are generally displayed 3D depictions anyways—i.e. see [46]. So we are presented with a representation problem: *how do we encode  $X$  within a 3D-PPSS?* Our selected solution is to employ the 2D-PPSSs of  $X$  as complex-valued arguments to some well-defined function that returns a real-valued output. This output will correspond to an *effective PPS* and serve as a *third* coordinate component to represent the topological deformations of  $X$  in a 3D-PPSS. Thus, with these tools we can define 3D-PPSSs for a 4D space-time, which are expressed in terms of well-defined generalized coordinates that *synchronize* the 3D Gullstrand-Painlevé-coordinates for the Schwarzschild metric, namely *3D GPS-coordinates*, and *3D Cartesian-coordinates* in a single *interconnected* system of *3D Riemannian-coordinates*. Again, recall that all of this is designed to enhance and generalize the definitions of [32].

Therefore, we let  $X$  be deformed within a 3D-PPSS and 3D real manifold  $Y$ , where  $X \subset Y$ . We define a 3D-PPS  $\vec{y} \in Y$  in the 3D-PPSS  $Y$  as a *triplex number*, *3-number*, *3-scalar*, and *3-vector* that simultaneously encodes a 2D location on  $X$  and a 3D location

on  $Y$ , where

$$\vec{y} \equiv \vec{y}_{\mathbb{R}} + \vec{y}_{\mathbb{I}} + \vec{y}_Z = \vec{x} + f(\vec{x}), \quad \forall \vec{x} \in X, \quad \forall \vec{y} \in Y, \quad (29)$$

with the *effective 3D-PPS* mapping constraints

$$\begin{aligned} \vec{y}_{\mathbb{R}} &\equiv \vec{x}_{\mathbb{R}} \\ \vec{y}_{\mathbb{I}} &\equiv \vec{x}_{\mathbb{I}} \\ \vec{y}_Z &\equiv f(\vec{x}) = f(\vec{x}_{\mathbb{R}} + \vec{x}_{\mathbb{I}}) \end{aligned} \quad (30)$$

for the generic *effective 3D-PPS function*  $f$ . Simply put,  $\vec{y}$  is a state within the state space  $Y$ . From there,  $f$  is extended to the *effective 3D-PPS GPS-coordinate function*  $f_{GPS} : X \rightarrow [0, 2\pi]$  and the *effective 3D-PPS Cartesian-coordinate function*  $f_{CART} : X \rightarrow [-\infty_Z, \infty_Z]$ . Hence, we augment eq. (29) with its corresponding *3D-PPS Riemannian-coordinate*, which identifies a

- *1D-PPS Triplex-coordinate* with component

1. *triplex-PPS*, namely  $\vec{y} \in Y$ ,

for

$$\vec{y} \equiv (\vec{y}) = (\vec{y}_{\mathbb{R}} + \vec{y}_{\mathbb{I}} + \vec{y}_Z), \quad \forall \vec{y} \in Y; \quad (31)$$

- *3D-PPS GPS-coordinate* (or “3D-PPS Spherical-coordinate”) with components

1. *amplitude-PPS* (“radius” or “modulus”), namely  $|\vec{y}| \in [0, \infty_{\mathbb{R}}]$ ,
2. *phase-PPS* (“azimuth”), namely  $\langle \vec{y} \rangle$ , namely  $\langle \vec{y} \rangle \in [0, 2\pi]$ , and
3. *inclination-PPS* (“zenith”), namely  $[\vec{y}] \in [0, 2\pi]$ , where  $f_{GPS}(\vec{x}) = [\vec{y}]$ ,

for

$$\vec{y} \equiv (|\vec{y}|, \langle \vec{y} \rangle, [\vec{y}]), \quad \forall \vec{y} \in Y; \quad (32)$$

and

- *3D-PPS Cartesian-coordinate* (or “3D-PPS Box-coordinate”) with components

1. *real-PPS* (“ $\mathbb{R}$ ” or “ $x$ ”), namely  $\vec{y}_{\mathbb{R}}$ , such that  $\vec{y}_{\mathbb{R}} \in [-\infty_{\mathbb{R}}, \infty_{\mathbb{R}}]$ ,
2. *imaginary-PPS* (“ $\mathbb{I}$ ” or “ $y$ ”), namely  $\vec{y}_{\mathbb{I}}$ , such that  $\vec{y}_{\mathbb{I}} \in [-\infty_{\mathbb{I}}, \infty_{\mathbb{I}}]$ , and
3. *projected-PPS* (“ $Z$ ” or “ $z$ ”), namely  $\vec{y}_Z$ , where  $f_{CART}(\vec{x}) = [\vec{y}]$ , such that  $\vec{y}_Z \in [-\infty_Z, \infty_Z]$ ,

for

$$\vec{y} \equiv (\vec{y}_{\mathbb{R}}, \vec{y}_{\mathbb{I}}, \vec{y}_Z), \quad \forall \vec{y} \in Y, \quad (33)$$

with the synchronizing Pythagorean and trigonometric interconnection constraints

$$\begin{aligned}
 |\vec{y}| &\equiv \sqrt{\vec{y}_R^2 + \vec{y}_I^2 + \vec{y}_Z^2} \\
 \langle \vec{y} \rangle &\equiv \arctan\left(\frac{\vec{y}_I}{\vec{y}_R}\right) \\
 [\vec{y}] &\equiv \arccos\left(\frac{\vec{y}_Z}{|\vec{y}|}\right)
 \end{aligned} \tag{34}$$

to define the 3D-PPS Riemannian-coordinate

$$\vec{y} \equiv (\vec{y}) = (|\vec{y}|, \langle \vec{y} \rangle, [\vec{y}]) = (\vec{y}_R, \vec{y}_I, \vec{y}_Z), \quad \forall \vec{y} \in Y, \tag{35}$$

which can be arranged into the row-vectors

$$\vec{y} \equiv [|\vec{y}|, \langle \vec{y} \rangle, [\vec{y}]] = [\vec{y}_R, \vec{y}_I, \vec{y}_Z] \tag{36}$$

and the column-vectors

$$\vec{y} \equiv \begin{bmatrix} |\vec{y}| \\ \langle \vec{y} \rangle \\ [\vec{y}] \end{bmatrix} = \begin{bmatrix} \vec{y}_R \\ \vec{y}_I \\ \vec{y}_Z \end{bmatrix} \tag{37}$$

for matrix notation.

*So what notation do we use to represent multiple 3D-PPSs in Y?* Well, for  $n$  3D-PPSs we can use numerical characters as additional subscripts to simply extend the notation of eq. (35) and generalize the 2D-PPSS formulation of eq. (11) to 3D-PPSS. Thus, using eq. (35) we may express the ordered set  $\{\vec{y}_1, \vec{y}_2, \dots, \vec{y}_n\} \subset Y$  for  $n$  distinct 3D-PPSs with the respective 3D Riemannian-coordinates

$$\begin{aligned}
 1 : \vec{y}_1 &= (\vec{y}_1) = (|\vec{y}_1|, \langle \vec{y}_1 \rangle, [\vec{y}_1]) = (\vec{y}_{1R}, \vec{y}_{1I}, \vec{y}_{1Z}) \\
 2 : \vec{y}_2 &= (\vec{y}_2) = (|\vec{y}_2|, \langle \vec{y}_2 \rangle, [\vec{y}_2]) = (\vec{y}_{2R}, \vec{y}_{2I}, \vec{y}_{2Z}) \\
 &\dots \\
 n : \vec{y}_n &= (\vec{y}_n) = (|\vec{y}_n|, \langle \vec{y}_n \rangle, [\vec{y}_n]) = (\vec{y}_{nR}, \vec{y}_{nI}, \vec{y}_{nZ}).
 \end{aligned} \tag{38}$$

To calculate the product of two triplex numbers, say  $\vec{y}_1$  and  $\vec{y}_2$ , see the triple multiplication definitions in the upcoming examples of Section 4.1.

*So how can we adjust T so it is consistent with Y in a 4D space-time?* Well, all we need to do is extend the  $T$  in eq. (13) from a topological circle (that is simultaneously dual to the interconnected  $X_-$  and  $X_+$  sub-surfaces in eq. (14)) to a topological Riemannian circle [38] (that is simultaneously dual to the interconnected  $Y_-$  and  $Y_+$  3-branes) with the amplitude-radius and amplitude-modulus  $\epsilon$ . To upgrade the topological definitions [32], we generalize eq. (12) to  $Y$  and use “3D zone trichotomy” to simultaneously define the 3D micro space zone  $Y_-$  and the 3D macro space zone  $Y_+$ ;  $T$  is dual to both  $Y_-$  and  $Y_+$  3-branes to establish a 4D space-time that generalizes [32]. Thus,  $\forall \vec{y} \in Y$  we know that precisely one of the following conditions must be satisfied

$$\begin{aligned}
 |\vec{y}| < \epsilon &\Leftrightarrow \vec{y} \in Y_- \subset Y \\
 |\vec{y}| = \epsilon &\Leftrightarrow \vec{y} \in T \subset Y \\
 |\vec{y}| > \epsilon &\Leftrightarrow \vec{y} \in Y_+ \subset Y,
 \end{aligned} \tag{39}$$

which generalizes eq. (12), where clearly  $Y_- \cap T = T \cap Y_+ = Y_- \cap Y_+ = \emptyset$  and  $Y_- \cup T \cup Y_+ = Y$ . Hence, the  $T$  of eq. (13) is projected to the multiplicative group of all non-zero 3D-PPSS

$$T \equiv \{\vec{y} \in Y : |\vec{y}| = \epsilon\}, \quad (40)$$

while the  $X_-$  and  $X_+$  of eq. (14) are respectively extended to the 3-branes

$$\begin{aligned} Y_- &\equiv \{\vec{y} \in Y : |\vec{y}| < \epsilon\} \\ Y_+ &\equiv \{\vec{y} \in Y : |\vec{y}| > \epsilon\}. \end{aligned} \quad (41)$$

So clearly eqs. (15–16) are generalized to

$$\epsilon \equiv |\vec{y}| = \sqrt{y_{\mathbb{R}}^2 + y_{\mathbb{I}}^2 + y_{\mathbb{Z}}^2}, \quad \forall \vec{y} \in T, \quad (42)$$

$$|\vec{y}| = \sqrt{y_{\mathbb{R}}^2 + y_{\mathbb{I}}^2 + y_{\mathbb{Z}}^2}, \quad \forall \vec{y} \in Y. \quad (43)$$

Therefore,  $T$  is isometrically embedded in  $Y$  with the one-to-one holographic mappings  $g : T \hookrightarrow Y$  and  $g : T \rightarrow Y_- \cup Y_+$  with the dual simultaneous bijections

$$\begin{aligned} {}^{3D}g_{time} : Y_- &\leftrightarrow T \hookrightarrow Y_+ \\ {}^{3D}g_{space} : Y_- &\hookrightarrow T \leftrightarrow Y_+ \end{aligned} \quad (44)$$

for our *dual* 4D space-time that generalize eq. (17). Hence,  $T$  is a common 2D surface boundary [47] that interconnects the dual  $Y_-$  and  $Y_+$  3-branes of [32]. All the 3D properties of  $Y_- \cup Y_+$  are inferred directly from the 2D properties of  $T$  as in [32]; this is consistent with the holographic principle in [10, 11, 12].

At this point, we've successfully defined the Riemannian dual 4D space-time topology; this is a direct upgrade to the topological framework of [32].

### 3.2 The 3D order parameter state space

$\forall \vec{y} \in Y$ , we may assign one or more 3D-OPSS layers, where each layer corresponds to a distinct 3D-OPSS with a spontaneously selected 3D-OPS. Following [32], these quantifiable features may represent fractional statistics and are expressed using a notation that is virtually identical to the 3D-PPS (and 3D-PPSS) eqs. (31–37) from the previous section. To illustrate the base case, we opt to assign one generic OPS layer to  $Y$  to encode one type of feature. Hence, at the 3D-PPS  $\vec{y} \in Y$  we have the single generic 3D-OPS  $\vec{\psi}(\vec{y})$  in the 3D-OPSS  $\Phi(\vec{y})$ , where  $\vec{\psi}(\vec{y}) \in \Phi(\vec{y})$ , such that  $\Phi(\vec{y})$  is the continuous and infinite set of 3D-OPSs (with cardinality  $|\Phi(\vec{y})| = \infty$ ) that is localized at  $\vec{y} \in Y$ . Therefore, we define

$$\vec{\psi}(\vec{y}) \equiv \vec{\psi}(\vec{y})_{\mathbb{R}} + \vec{\psi}(\vec{y})_{\mathbb{I}} + \vec{\psi}(\vec{y})_{\mathbb{Z}}, \quad \forall \vec{y} \in Y, \quad \forall \vec{\psi}(\vec{y}) \in \Phi(\vec{y}), \quad (45)$$

which is expressed in the *3D-OPS Riemannian-vector* notation that synchronizes and simultaneously references three vector systems. Simply put,  $\vec{\psi}(\vec{y})$  is a state in the state space  $\Phi(\vec{y})$ . Thus, to augment eq. (45) we use the 1D-PPS Triplex-coordinate notation of eq. (31) to construct the *1D-OPS Triplex-vector*

$$\vec{\psi}(\vec{y}) \equiv (\vec{\psi}(\vec{y})) = (\vec{\psi}(\vec{y})_{\mathbb{R}} + \vec{\psi}(\vec{y})_{\mathbb{I}} + \vec{\psi}(\vec{y})_{\mathbb{Z}}), \quad \forall \vec{\psi}(\vec{y}) \in \Phi(\vec{y}). \quad (46)$$

Similarly, we use the 3D-PPS GPS-coordinate notation of eq. (32) to construct the *3D-OPS GPS-vector* (or “3D-OPS Spherical-vector”)

$$\vec{\psi}(\vec{y}) \equiv (|\vec{\psi}(\vec{y})|, \langle \vec{\psi}(\vec{y}) \rangle, [\vec{\psi}(\vec{y})]), \quad \forall \vec{\psi}(\vec{y}) \in \Phi(\vec{y}), \quad (47)$$

with components *amplitude-OPS*  $|\vec{\psi}(\vec{y})| \in [0, \infty_{\mathbb{R}}]$ , *phase-OPS*  $\langle \vec{\psi}(\vec{y}) \rangle \in [0, 2\pi]$ , and *inclination-OPS*  $[\vec{\psi}(\vec{y})] \in [0, 2\pi]$ , respectively. Subsequently, we use the 3D-PPS Cartesian-coordinate notation of eq. (33) to construct the *3D-OPS Cartesian-vector* (or “3D-OPS Box-vector”)

$$\vec{\psi}(\vec{y}) \equiv (\vec{\psi}(\vec{y})_{\mathbb{R}}, \vec{\psi}(\vec{y})_{\mathbb{I}}, \vec{\psi}(\vec{y})_Z), \quad \forall \vec{\psi}(\vec{y}) \in \Phi(\vec{y}), \quad (48)$$

with components *real-OPS*  $\vec{\psi}(\vec{y})_{\mathbb{R}} \in [-\infty_{\mathbb{R}}, \infty_{\mathbb{R}}]$ , *imaginary-OPS*  $\vec{\psi}(\vec{y})_{\mathbb{I}} \in [-\infty_{\mathbb{I}}, \infty_{\mathbb{I}}]$ , and *projected-OPS*  $\vec{\psi}(\vec{y})_Z \in [-\infty_Z, \infty_Z]$ , respectively. Eqs. (46–48) satisfy the synchronizing Pythagorean and trigonometric interconnection constraints

$$\begin{aligned} |\vec{\psi}(\vec{y})| &\equiv \sqrt{\vec{\psi}^2(\vec{y})_{\mathbb{R}} + \vec{\psi}^2(\vec{y})_{\mathbb{I}} + \vec{\psi}^2(\vec{y})_Z} \\ \langle \vec{\psi}(\vec{y}) \rangle &\equiv \arctan\left(\frac{\vec{\psi}(\vec{y})_{\mathbb{I}}}{\vec{\psi}(\vec{y})_{\mathbb{R}}}\right) \\ [\vec{\psi}(\vec{y})] &\equiv \arccos\left(\frac{\vec{\psi}(\vec{y})_Z}{|\vec{\psi}(\vec{y})|}\right) \end{aligned} \quad (49)$$

to define the 3D-OPS Riemannian-vector

$$\vec{\psi}(\vec{y}) \equiv (\vec{\psi}(\vec{y})) = (|\vec{\psi}(\vec{y})|, \langle \vec{\psi}(\vec{y}) \rangle, [\vec{\psi}(\vec{y})]) = (\vec{\psi}(\vec{y})_{\mathbb{R}}, \vec{\psi}(\vec{y})_{\mathbb{I}}, \vec{\psi}(\vec{y})_Z), \quad \forall \vec{\psi}(\vec{y}) \in \Phi(\vec{y}), \quad (50)$$

which can be arranged into the row-vectors

$$\vec{\psi}(\vec{y}) \equiv [|\vec{\psi}(\vec{y})|, \langle \vec{\psi}(\vec{y}) \rangle, [\vec{\psi}(\vec{y})]] = [\vec{\psi}(\vec{y})_{\mathbb{R}}, \vec{\psi}(\vec{y})_{\mathbb{I}}, \vec{\psi}(\vec{y})_Z] \quad (51)$$

and the column-vectors

$$\vec{\psi}(\vec{y}) \equiv \begin{bmatrix} |\vec{\psi}(\vec{y})| \\ \langle \vec{\psi}(\vec{y}) \rangle \\ [\vec{\psi}(\vec{y})] \end{bmatrix} = \begin{bmatrix} \vec{\psi}(\vec{y})_{\mathbb{R}} \\ \vec{\psi}(\vec{y})_{\mathbb{I}} \\ \vec{\psi}(\vec{y})_Z \end{bmatrix} \quad (52)$$

for matrix notation.

Next, similarly to eq. (26), we define the various types of 3D-OPSs that give us extreme flexibility for encoding the topological deformations and wavefunctions of [32] with an additional degree of freedom. For this, we can employ 3D-OPSs to represent the *specific* quantum number deformation states as in [32] or to represent more *general* deformation state that may be applied to other physics frameworks. For example, if we wish to specifically encode the quantum number states of magnetic charge, electric charge, color charge, isospin, orbital angular momentum, spin angular momentum, and total angular momentum for a 3D-OPS

version of the baryon topological deformations, wavefunctions, and tensors in [32], then we can apply eq. (50)  $\forall \vec{y} \in Y$  to define the respective specific 3D-OPSS (in short form) as

$$\begin{aligned}
 \vec{\psi}_B(\vec{y}) &\equiv (\vec{\psi}_B(\vec{y})), \quad \forall \vec{\psi}_B(\vec{y}) \in \Phi_B(\vec{y}) \\
 \vec{\psi}_E(\vec{y}) &\equiv (\vec{\psi}_E(\vec{y})), \quad \forall \vec{\psi}_E(\vec{y}) \in \Phi_E(\vec{y}) \\
 \vec{\psi}_C(\vec{y}) &\equiv (\vec{\psi}_C(\vec{y})), \quad \forall \vec{\psi}_C(\vec{y}) \in \Phi_C(\vec{y}) \\
 \vec{\psi}_I(\vec{y}) &\equiv (\vec{\psi}_I(\vec{y})), \quad \forall \vec{\psi}_I(\vec{y}) \in \Phi_I(\vec{y}) \\
 \vec{\psi}_L(\vec{y}) &\equiv (\vec{\psi}_L(\vec{y})), \quad \forall \vec{\psi}_L(\vec{y}) \in \Phi_L(\vec{y}) \\
 \vec{\psi}_S(\vec{y}) &\equiv (\vec{\psi}_S(\vec{y})), \quad \forall \vec{\psi}_S(\vec{y}) \in \Phi_S(\vec{y}) \\
 \vec{\psi}_J(\vec{y}) &\equiv (\vec{\psi}_J(\vec{y})), \quad \forall \vec{\psi}_J(\vec{y}) \in \Phi_J(\vec{y})
 \end{aligned} \tag{53}$$

Moreover, if we wish to encode topological deformation states without a specific reference to quantum numbers, then we can similarly apply eq. (50) to define the general and “generic” 3D-OPS as

$$\vec{\psi}_{\rightarrow}(\vec{y}_1) \equiv (\vec{\psi}_{\rightarrow}(\vec{y}_1)), \quad \forall \vec{\psi}_{\rightarrow}(\vec{y}_1) \in \Phi_{\rightarrow}(\vec{y}_1), \quad \forall \vec{y}_1 \in Y, \tag{54}$$

such that

$$\vec{y}_2 \equiv \vec{y}_1 + \vec{\psi}_{\rightarrow}(\vec{y}_1) \tag{55}$$

is the *effective 3D-PPS*  $\vec{y}_2 \in Y$  that is identified by the deformation  $\vec{\psi}_{\rightarrow}(\vec{y}_1)$ . See Table 4 for a list of possible 3D-OPS candidates that we may (or may not) opt to use in the dual 4D space-time. The triplex multiplication definitions in the upcoming examples of Section 4.1 are pertinent to this 3D-OPS implementation. Consequently, this 3D-OPS multiplication is applied to the multiple 3D-OPSS comprising the wavefunctions and tensors in the upcoming examples of Section 4.2.

Table 4: A list of possible 3D-OPS candidates designed to encode topological deformation and wavefunction states in the dual 4D space-time.

Name	Symbol	3D Order Parameter State	Application
Magnetic Charge	$B$	$\vec{\psi}_B(\vec{y}) \equiv \vec{\psi}_B(\vec{y})_{\mathbb{R}} + \vec{\psi}_B(\vec{y})_{\mathbb{I}} + \vec{\psi}_B(\vec{y})_Z$	Specific
Electric Charge	$E$	$\vec{\psi}_E(\vec{y}) \equiv \vec{\psi}_E(\vec{y})_{\mathbb{R}} + \vec{\psi}_E(\vec{y})_{\mathbb{I}} + \vec{\psi}_E(\vec{y})_Z$	Specific
Color Charge	$C$	$\vec{\psi}_C(\vec{y}) \equiv \vec{\psi}_C(\vec{y})_{\mathbb{R}} + \vec{\psi}_C(\vec{y})_{\mathbb{I}} + \vec{\psi}_C(\vec{y})_Z$	Specific
Isospin	$I$	$\vec{\psi}_I(\vec{y}) \equiv \vec{\psi}_I(\vec{y})_{\mathbb{R}} + \vec{\psi}_I(\vec{y})_{\mathbb{I}} + \vec{\psi}_I(\vec{y})_Z$	Specific
Orbital Angular Momentum	$L$	$\vec{\psi}_L(\vec{y}) \equiv \vec{\psi}_L(\vec{y})_{\mathbb{R}} + \vec{\psi}_L(\vec{y})_{\mathbb{I}} + \vec{\psi}_L(\vec{y})_Z$	Specific
Spin Angular Momentum	$S$	$\vec{\psi}_S(\vec{y}) \equiv \vec{\psi}_S(\vec{y})_{\mathbb{R}} + \vec{\psi}_S(\vec{y})_{\mathbb{I}} + \vec{\psi}_S(\vec{y})_Z$	Specific
Total Angular Momentum	$J$	$\vec{\psi}_J(\vec{y}) \equiv \vec{\psi}_J(\vec{y})_{\mathbb{R}} + \vec{\psi}_J(\vec{y})_{\mathbb{I}} + \vec{\psi}_J(\vec{y})_Z$	Specific
“Generic” Deformation	$\rightarrow$	$\vec{\psi}_{\rightarrow}(\vec{y}) \equiv \vec{\psi}_{\rightarrow}(\vec{y})_{\mathbb{R}} + \vec{\psi}_{\rightarrow}(\vec{y})_{\mathbb{I}} + \vec{\psi}_{\rightarrow}(\vec{y})_Z$	General

At this point, we’ve assembled the triplex information structures and encoding methodology for our 4D space-time, where each 3D-PPS in the 3D-PPSS is equipped with a localized 3D-OPSS—recall Table 3. This is a direct upgrade to the spontaneous symmetry breaking framework of [32]. See Table 5 for a brief recapitulation of the generic complex and triplex information structures.

Table 5: A summary of the complex and triplex information structures for our dual 3D and 4D space-time topologies, respectively.

Name	Value	Represents	Type
2D-PPS	$\vec{x} \in X \subset Y$	Location	Coordinate
2D-PPSS	$X \subset Y$	Location Space	Coordinate Space
2D-OPS	$\vec{\psi}(\vec{x}) \in \Phi(\vec{x})$	Feature	Vector
2D-OPSS	$\Psi(\vec{x})$	Feature Space	Vector Space
3D-PPS	$\vec{y} \in Y$	Location	Coordinate
3D-PPSS	$Y$	Location Space	Coordinate Space
3D-OPS	$\vec{\psi}(\vec{y}) \in \Phi(\vec{y})$	Feature	Vector
3D-OPSS	$\Psi(\vec{y})$	Feature Space	Vector Space

## 4 Example applications

In this section, we provide three distinct and introductory examples that apply the encoding framework to fractal geometry, particle physics, and astro physics.

### 4.1 A brief correspondence to White and Nylander on triplex fractals and computer graphics

Here, the objective is to apply the triplex framework of Section 3 to nullify the White-Nylander mythical beast. This wild beast has been cornered by D. White and P. Nylander—the pioneers that have developed a triplex algebra to encode triplex fractals for computer graphics [33, 34, 35]. A triplex algebra is an arithmetic for 3D coordinates and is a prerequisite for calculating 3D fractals [33, 34, 35]. A prime expression of this chaotic beast is the Mandelbulb [33, 34, 35]—a 3D equivalent of B. Mandelbrot’s set [7]. D. White and P. Nylander extended complex multiplication to define triplex multiplication (and hence triplex exponentiation) but the beast still exists because of two constrictions [33, 34, 35]:

1. the triplex polar form is not unique, and
2. the triplex algebra is not well-behaved.

Thus, in order to finish the beast and upgrade the existing triplex operators we must use the triplex framework of Section 3 to identify:

1. a triplex polar form that is unique, and
2. a triplex algebra that is well-behaved.

So we use the triplex framework of Section 3 to approach the beast from distinct two perspectives. First, we consider the White-Nylander approach with the former conditions, and second, we consider an alternative approach with the latter conditions.

#### 4.1.1 The White-Nylander approach

This first approach contains no new ideas; it simply prepares for our second approach by putting the captivating work of D. White and P. Nylander [33, 34, 35] in the context of our encoding framework.

Our departure begins by considering two complex numbers in *conventional* polar form of [33, 34, 35], namely  $\vec{x}_1$  and  $\vec{x}_2$ , where  $|\vec{x}_1|$  and  $|\vec{x}_2|$  are the amplitude-PPSs while  $\langle\vec{x}_1\rangle$  and  $\langle\vec{x}_2\rangle$  are the phase-PPSs in eq. (23). Using our 2D-PPS notation of Section 2, the product of  $\vec{x}_1$  and  $\vec{x}_2$  is  $|\vec{x}_1||\vec{x}_2|e^{i(\langle\vec{x}_1\rangle+\langle\vec{x}_2\rangle)}$  [33, 34, 35]—the complex multiplication comprises two operations [33, 34, 35]:

1. stretching  $\vec{x}_1$  by the amplitude-PPS (modulus)  $|\vec{x}_2|$ , and
2. rotating  $\vec{x}_1$  by the phase-PPS  $\langle\vec{x}_2\rangle$ .

Now, using eq. (35) we let  $\vec{y}$  be an arbitrary 3D-PPS in the 3D-PPSS  $Y$ . In this initial example, the phase-PPS  $\langle\vec{x}_1\rangle$  will be supplied as the angle parameter to the rotational matrices of [33, 34, 35] to swivel  $\vec{y}$  around the three axes of  $Y$ . So in terms of [33, 34, 35] and the supplied the angle parameter  $\langle\vec{x}_1\rangle$ , there are three basic rotation matrices that correspond to swivels about the  $\mathbb{R}$ -axis,  $\mathbb{I}$ -axis, and  $Z$ -axis of  $Y$ , which are

$$R_{\mathbb{R}}(\langle\vec{x}_1\rangle) = \begin{pmatrix} 1 & 0 & 0 \\ 0 & \cos\langle\vec{x}_1\rangle & -\sin\langle\vec{x}_1\rangle \\ 0 & \sin\langle\vec{x}_1\rangle & \cos\langle\vec{x}_1\rangle \end{pmatrix}, \quad (56)$$

$$R_{\mathbb{I}}(\langle\vec{x}_1\rangle) = \begin{pmatrix} \cos\langle\vec{x}_1\rangle & 0 & \sin\langle\vec{x}_1\rangle \\ 0 & 1 & 0 \\ -\sin\langle\vec{x}_1\rangle & 0 & \cos\langle\vec{x}_1\rangle \end{pmatrix}, \quad (57)$$

and

$$R_Z(\langle\vec{x}_1\rangle) = \begin{pmatrix} \cos\langle\vec{x}_1\rangle & -\sin\langle\vec{x}_1\rangle & 0 \\ \sin\langle\vec{x}_1\rangle & \cos\langle\vec{x}_1\rangle & 0 \\ 0 & 0 & 1 \end{pmatrix}, \quad (58)$$

respectively. Here, eqs. (56–58) correspond to the rotations [33, 34, 35]

$$R_{\mathbb{R}}(\langle\vec{x}_1\rangle) : (\vec{y}_{\mathbb{R}}, \vec{y}_{\mathbb{I}}, \vec{y}_Z) \mapsto (\vec{y}_{\mathbb{R}}, \vec{y}_{\mathbb{I}} \cos\langle\vec{x}_1\rangle - \vec{y}_Z \sin\langle\vec{x}_1\rangle, \vec{y}_{\mathbb{I}} \sin\langle\vec{x}_1\rangle + \vec{y}_Z \cos\langle\vec{x}_1\rangle), \quad (59)$$

$$R_{\mathbb{I}}(\langle\vec{x}_1\rangle) : (\vec{y}_{\mathbb{R}}, \vec{y}_{\mathbb{I}}, \vec{y}_Z) \mapsto (\vec{y}_{\mathbb{R}} \cos\langle\vec{x}_1\rangle + \vec{y}_Z \sin\langle\vec{x}_1\rangle, \vec{y}_{\mathbb{I}}, \vec{y}_Z \cos\langle\vec{x}_1\rangle - \vec{y}_{\mathbb{R}} \sin\langle\vec{x}_1\rangle), \quad (60)$$

and

$$R_Z(\langle\vec{x}_1\rangle) : (\vec{y}_{\mathbb{R}}, \vec{y}_{\mathbb{I}}, \vec{y}_Z) \mapsto (\vec{y}_{\mathbb{R}} \cos\langle\vec{x}_1\rangle - \vec{y}_{\mathbb{I}} \sin\langle\vec{x}_1\rangle, \vec{y}_{\mathbb{R}} \sin\langle\vec{x}_1\rangle + \vec{y}_{\mathbb{I}} \cos\langle\vec{x}_1\rangle, \vec{y}_Z), \quad (61)$$

respectively. The identified

$$\begin{aligned} &(\vec{y}_{\mathbb{R}}, \vec{y}_{\mathbb{I}} \cos\langle\vec{x}_1\rangle - \vec{y}_Z \sin\langle\vec{x}_1\rangle, \vec{y}_{\mathbb{I}} \sin\langle\vec{x}_1\rangle + \vec{y}_Z \cos\langle\vec{x}_1\rangle) \\ &(\vec{y}_{\mathbb{R}} \cos\langle\vec{x}_1\rangle + \vec{y}_Z \sin\langle\vec{x}_1\rangle, \vec{y}_{\mathbb{I}}, \vec{y}_Z \cos\langle\vec{x}_1\rangle - \vec{y}_{\mathbb{R}} \sin\langle\vec{x}_1\rangle) \\ &(\vec{y}_{\mathbb{R}} \cos\langle\vec{x}_1\rangle - \vec{y}_{\mathbb{I}} \sin\langle\vec{x}_1\rangle, \vec{y}_{\mathbb{R}} \sin\langle\vec{x}_1\rangle + \vec{y}_{\mathbb{I}} \cos\langle\vec{x}_1\rangle, \vec{y}_Z) \end{aligned} \quad (62)$$

results of eqs. (59–61) come from the corresponding matrix multiplication of  $R_{\mathbb{R}}(\langle \vec{x}_1 \rangle)$ ,  $R_{\mathbb{I}}(\langle \vec{x}_1 \rangle)$ , and  $R_Z(\langle \vec{x}_1 \rangle)$  by the vector  $(\vec{y}_{\mathbb{R}}, \vec{y}_{\mathbb{I}}, \vec{y}_Z)$  interpreted as a matrix with one vertical column [33, 34, 35].

Next, we consider the secondary rotation angle  $\langle \vec{x}_2 \rangle$ . Upon simultaneously considering the two angle parameters  $\langle \vec{x}_1 \rangle$  and  $\langle \vec{x}_2 \rangle$  for rotation eqs. (59–61), we take into account all pairwise products of the rotational matrices in eqs. (56–58) to obtain the six distinct matrix terms

$$\begin{aligned}
 &R_{\mathbb{R}}(\langle \vec{x}_1 \rangle)R_{\mathbb{I}}(\langle \vec{x}_2 \rangle) \\
 &R_{\mathbb{I}}(\langle \vec{x}_1 \rangle)R_{\mathbb{R}}(\langle \vec{x}_2 \rangle) \\
 &R_Z(\langle \vec{x}_1 \rangle)R_{\mathbb{I}}(\langle \vec{x}_2 \rangle) \\
 &R_{\mathbb{I}}(\langle \vec{x}_1 \rangle)R_Z(\langle \vec{x}_2 \rangle) \\
 &R_Z(\langle \vec{x}_1 \rangle)R_{\mathbb{R}}(\langle \vec{x}_2 \rangle) \\
 &R_{\mathbb{R}}(\langle \vec{x}_1 \rangle)R_Z(\langle \vec{x}_2 \rangle),
 \end{aligned} \tag{63}$$

where each is interpreted as a rotation through the *two* angles [33, 34, 35] in  $Y$ . Applying each of the six matrix results of eq. (63) is analogous to multiplying two triplex numbers [33, 34, 35]. Thus, in order to acquire the actual formulas for triplex multiplication, we multiply the matrix products of eq. (63) by the vectors  $(1, 0, 0)$ ,  $(0, 1, 0)$ , and  $(0, 0, 1)$  [33, 34, 35]—the three resulting triplex numbers are the three columns of the matrix [33, 34, 35]. Now in the context of generating graphics in  $Y$ , only two of these triplex values are of interest in each matrix product because the ones that have zero terms are degenerate from a graphical perspective [33, 34, 35]. So although these steps are relatively intuitive thus far, this is where the beast’s expression begins to exhibit convolution because we’ve acquired 12 relevant triplex polar forms and now we must additionally attempt all combinations of minus and plus for  $\langle \vec{x}_1 \rangle$  and  $\langle \vec{x}_2 \rangle$  to yield a total of 48 distinct formulas for the triplex polar form [33, 34, 35]. Moreover, it is suggested in [35] that we interchange  $\langle \vec{x}_1 \rangle$  and  $\langle \vec{x}_2 \rangle$  to generate a total of 96 possibilities. Here, each variation is an effective formula for the triplex polar form, which is similar to P. Nylander’s [33, 34, 35]

$$(\cos\langle \vec{x}_1 \rangle \cos\langle \vec{x}_2 \rangle, \sin\langle \vec{x}_1 \rangle \cos\langle \vec{x}_2 \rangle, \sin\langle \vec{x}_2 \rangle). \tag{64}$$

For instance, any complex number, such as  $\vec{x}_1$ , can be raised to a real power  $p$  by employing  $(|\vec{x}_1|e^{i\langle \vec{x}_1 \rangle})^p = |\vec{x}_1|^p e^{pi\langle \vec{x}_1 \rangle}$  [33, 34, 35]. By analogy, the triplex exponentiation formulation is identified in [33, 34, 35] as

$$(\vec{y}_{\mathbb{R}}, \vec{y}_{\mathbb{I}}, \vec{y}_Z)^p = |\vec{y}|^p (\cos(p\langle \vec{x}_1 \rangle) \cos(p\langle \vec{x}_2 \rangle), \sin(p\langle \vec{x}_1 \rangle) \cos(p\langle \vec{x}_2 \rangle), \sin(p\langle \vec{x}_2 \rangle)), \tag{65}$$

with the constraints

$$\begin{aligned}
 |\vec{y}| &= \sqrt{\vec{y}_{\mathbb{R}}^2 + \vec{y}_{\mathbb{I}}^2 + \vec{y}_Z^2} \\
 \langle \vec{y} \rangle &= \langle \vec{x}_1 \rangle = \text{atan2}(\vec{y}_{\mathbb{I}}, \vec{y}_{\mathbb{R}}) \\
 [\vec{y}] &= \langle \vec{x}_2 \rangle = \arcsin\left(\frac{\vec{y}_Z}{|\vec{y}|}\right).
 \end{aligned} \tag{66}$$

According to [33, 34, 35]  $p$  can be any real value, so in addition to employing the natural numbers, one can also define negative and fractional powers.

Moreover, for a two arbitrary 3D-PPSs in the 3D-PPSS  $Y$ , namely  $\vec{y}_1$  and  $\vec{y}_2$ , the selected triplex polar form exhibits a multiplication formula similar to [33, 34, 35]

$$\begin{aligned}
 (\vec{y}_{1_R}, \vec{y}_{1_I}, \vec{y}_{1_Z}) \times (\vec{y}_{2_R}, \vec{y}_{2_I}, \vec{y}_{2_Z}) = |\vec{y}_1| |\vec{y}_2| ( & \\
 & \cos(\langle \vec{x}_1 \rangle + \langle \vec{x}_3 \rangle) \cos(\langle \vec{x}_2 \rangle + \langle \vec{x}_4 \rangle), \\
 & \sin(\langle \vec{x}_1 \rangle + \langle \vec{x}_3 \rangle) \cos(\langle \vec{x}_2 \rangle + \langle \vec{x}_4 \rangle), \quad (67) \\
 & \sin(\langle \vec{x}_2 \rangle + \langle \vec{x}_4 \rangle) \\
 & ),
 \end{aligned}$$

where

$$\begin{aligned}
 |\vec{y}_1| &= \sqrt{\vec{y}_{1_R}^2 + \vec{y}_{1_I}^2 + \vec{y}_{1_Z}^2} \\
 \langle \vec{y}_1 \rangle &= \langle \vec{x}_1 \rangle = \text{atan2}(\vec{y}_{1_I}, \vec{y}_{1_R}) \\
 [\vec{y}_1] &= \langle \vec{x}_2 \rangle = \arcsin\left(\frac{\vec{y}_{1_Z}}{|\vec{y}_1|}\right)
 \end{aligned} \quad (68)$$

and

$$\begin{aligned}
 |\vec{y}_2| &= \sqrt{\vec{y}_{2_R}^2 + \vec{y}_{2_I}^2 + \vec{y}_{2_Z}^2} \\
 \langle \vec{y}_2 \rangle &= \langle \vec{x}_3 \rangle = \text{atan2}(\vec{y}_{2_I}, \vec{y}_{2_R}) \\
 [\vec{y}_2] &= \langle \vec{x}_4 \rangle = \arcsin\left(\frac{\vec{y}_{2_Z}}{|\vec{y}_2|}\right),
 \end{aligned} \quad (69)$$

such that  $\vec{x}_1, \vec{x}_2, \vec{x}_3$ , and  $\vec{x}_4$  in the form eq. (7) correspond to the the relevant transformations. So in terms of [33, 34, 35], the selected polar form of P. Nylander’s eq. (64) is utilized in eqs. (65) and (67) for the sake of illustration simplicity—each polar form variant generates a different pair of formulas [33, 34, 35]. Thus, for the 48 distinct exponential combinations of these triplex numbers see the summarized results of T. Boniecki [35] and J. Rampe’s “Visions of Chaos” software [48].

At this point, we’ve provided the first approach with an introductory example on how the triplex framework of Section 3 can be applied to D. White and P. Nylander’s triplex algebra for the triplex fractals [33, 34, 35] in 3D-PPSS.

#### 4.1.2 An alternative approach

This second approach aims to finish the triplex multiplication aspect of the White-Nylander mythical beast [33, 34, 35]. Here, we hypothesize that complex multiplication can be extended to the triplex numbers with two conditions:

1. the triplex polar form is unique, and
2. the triplex numbers do form a well-behaved algebra.

For this, we propose that the triplex multiplication for  $\vec{y}_1$  and  $\vec{y}_2$  comprises three operations:

1. stretching  $\vec{y}_1$  by the amplitude-PPS  $|\vec{y}_2|$ ,
2. rotating  $\vec{y}_1$  by the phase-PPS  $\langle \vec{y}_2 \rangle$ , and
3. rotating  $\vec{y}_1$  by the inclination-PPS  $[\vec{y}_2]$ .

Thus, if we define the triplex product as

$$\vec{y}_3 \equiv \vec{y}_1 \vec{y}_2 \tag{70}$$

for  $\vec{y}_1, \vec{y}_2, \vec{y}_3 \in Y$ , then eq. (70) implies

$$\begin{aligned} |\vec{y}_3| &\equiv |\vec{y}_1| |\vec{y}_2| \\ \langle \vec{y}_3 \rangle &\equiv \langle \vec{y}_1 \rangle + \langle \vec{y}_2 \rangle \\ [\vec{y}_3] &\equiv [\vec{y}_1] + [\vec{y}_2]. \end{aligned} \tag{71}$$

From here, one can venture onward and employ eqs. (70–71) to further define the triplex exponentiation for triplex fractals such as the Mandelbulb [33, 34, 35]. To define triplex exponentiation, all we need to do is iterate the triplex multiplication of eqs. (70–71).

At this point, we’ve provided the second and alternative approach for an introductory example on how the triplex framework of Section 3 can be applied to D. White and P. Nylander’s triplex algebra and fractals [33, 34, 35] in 3D-PPSS.

#### 4.2 Color-anticolor confinement and baryon-antibaryon duality

Here, the triplex framework of Section 3 is applied to upgrade the fractional quantum number order parameters of the baryon wavefunction, antibaryon wavefunction, and anti-symmetric tensor in the analytic confinement and duality proof of [32] from 2D-OPSs to 3D-OPSs. For this, the triplex multiplication of Section 4.1 is employed.

Thus, following [32], for the baryon-antibaryon pairs that are confined to  $T$  of eq. (40) on the six-coloring kagome lattice of antiferromagnetic ordering, we define the baryon wavefunction for the three colored quark 3D-PPSSs, namely  $\{\vec{r}, \vec{g}, \vec{b}\} \subset T \subset Y$ , and the corresponding antibaryon wavefunction for the three anticolored antiquarks 3D-PPSSs, namely  $\{\vec{\bar{r}}, \vec{\bar{g}}, \vec{\bar{b}}\} \subset T \subset Y$ , in the upgraded Gribov QCD/QED vacuum, respectively. For this, we “Cooper pair” the set of strongly conserved quantum numbers, namely  $\{\vec{\psi}_C, \vec{\psi}_I, \vec{\psi}_J\}$ , to construct a strong baryon wavefunction constraint for the baryon-antibaryon confinement, duality, and antisymmetry of  $T$  [32], such that  $\vec{\psi}_J = \vec{\psi}_L + \vec{\psi}_S$  is the “ $B_{SO}$ -vector” of [49]. The  $q\bar{q}$  pairs confined to  $T$  on the six-coloring kagome lattice manifold are located at the 3D-PPSSs  $\vec{r}, \vec{g}, \vec{b}, \vec{\bar{r}}, \vec{\bar{g}}, \vec{\bar{c}} \in T$ . First, the encoded  $q\bar{q}$  states adhere to the uniformly-arranged

“phase-PPS *and* inclination-PPS constraints”

$$\begin{aligned}
\langle \vec{r} \rangle &\equiv \langle \vec{r} \rangle \pm \pi \\
\langle \vec{g} \rangle &\equiv \langle \vec{g} \rangle \pm \pi \\
\langle \vec{b} \rangle &\equiv \langle \vec{b} \rangle \pm \pi \\
[\vec{r}] &\equiv [\vec{r}] \pm \pi \\
[\vec{g}] &\equiv [\vec{g}] \pm \pi \\
[\vec{b}] &\equiv [\vec{b}] \pm \pi,
\end{aligned} \tag{72}$$

which update the 2D-PPS constraints of eq. (28) in [32] to the desired 3D-PPS configuration—see the *angle* components of the parity-transformation in the upcoming eq. (85) and the time-reversal in the upcoming eq. (86) for CPT-theorem compliance. Second, the encoded  $q\bar{q}$  states adhere to the uniformly-arranged “amplitude-PPS constraints”

$$|\vec{r}| \equiv |\vec{g}| \equiv |\vec{b}| \equiv |\vec{r}| \equiv |\vec{g}| \equiv |\vec{b}| \equiv \epsilon \tag{73}$$

so they exist within the  $T$  defined in eq. (40)—see the *amplitude* components of the parity-transformation in the upcoming eq. (85) and the time-reversal in the upcoming eq. (86) for CPT-theorem compliance. Third, the encoded  $q\bar{q}$  states adhere to the uniformly-arranged “phase-OPS *and* inclination-OPS antiferromagnetic ordering constraints”

$$\begin{aligned}
\langle \vec{\psi}_J(\vec{r}) \rangle &\equiv \langle \vec{\psi}_J(\vec{r}) \rangle \pm \pi \\
\langle \vec{\psi}_J(\vec{g}) \rangle &\equiv \langle \vec{\psi}_J(\vec{g}) \rangle \pm \pi \\
\langle \vec{\psi}_J(\vec{b}) \rangle &\equiv \langle \vec{\psi}_J(\vec{b}) \rangle \pm \pi \\
[\vec{\psi}_J(\vec{r})] &\equiv [\vec{\psi}_J(\vec{r})] \pm \pi \\
[\vec{\psi}_J(\vec{g})] &\equiv [\vec{\psi}_J(\vec{g})] \pm \pi \\
[\vec{\psi}_J(\vec{b})] &\equiv [\vec{\psi}_J(\vec{b})] \pm \pi,
\end{aligned} \tag{74}$$

which update the 2D-OPS constraints of eqs. (29–31) in [32] to the desired 3D-OPS configuration.

Next, by exercising eqs. (72–74) we update the *full* baryon and antibaryon states of eqs. (32–33) in [32] to

$$\vec{\Psi}_{total}(\vec{r}, \vec{g}, \vec{b}) \equiv \vec{\Psi}(\vec{r}) \times \vec{\Psi}(\vec{g}) \times \vec{\Psi}(\vec{b}) \tag{75}$$

$$\vec{\Psi}_{total}(\vec{r}, \vec{g}, \vec{b}) \equiv \vec{\Psi}(\vec{r}) \times \vec{\Psi}(\vec{g}) \times \vec{\Psi}(\vec{b}) \tag{76}$$

for a 3D-OPS version of the baryon-antibaryon confinement and duality. In eq. (75), the *red*, *green*, and *blue* colored wavefunctions of the baryon wavefunction  $\vec{\Psi}_{total}(\vec{r}, \vec{g}, \vec{b})$  that encode the quark features at  $\vec{r}, \vec{g}, \vec{b} \in T$  on the three-coloring triangular sub-lattice of eqs. (34–36) in [32] become

$$\begin{aligned}
\vec{\Psi}(\vec{r}) &\equiv \vec{\psi}_C(\vec{r}) \times \vec{\psi}_J(\vec{r}) \times \vec{\psi}_I(\vec{r}) \times \vec{r}, & \vec{\Psi}(\vec{r}) &\stackrel{def}{=} \langle \vec{r} | \vec{\Psi} \rangle, \\
\vec{\Psi}(\vec{g}) &\equiv \vec{\psi}_C(\vec{g}) \times \vec{\psi}_J(\vec{g}) \times \vec{\psi}_I(\vec{g}) \times \vec{g}, & \vec{\Psi}(\vec{g}) &\stackrel{def}{=} \langle \vec{g} | \vec{\Psi} \rangle, \\
\vec{\Psi}(\vec{b}) &\equiv \vec{\psi}_C(\vec{b}) \times \vec{\psi}_J(\vec{b}) \times \vec{\psi}_I(\vec{b}) \times \vec{b}, & \vec{\Psi}(\vec{b}) &\stackrel{def}{=} \langle \vec{b} | \vec{\Psi} \rangle,
\end{aligned} \tag{77}$$

while in eq. (76) the *antired*, *antigreen*, and *antiblue* anticolored wavefunctions of the antibaryon wavefunction  $\vec{\Psi}_{total}(\vec{r}, \vec{g}, \vec{b})$  that encode the antiquark features at  $\vec{r}, \vec{g}, \vec{b} \in T$  on the three-anticoloring triangular sub-lattice of eqs. (37–39) in [32] become

$$\begin{aligned}\vec{\Psi}(\vec{r}) &\equiv \vec{\psi}_C(\vec{r}) \times \vec{\psi}_J(\vec{r}) \times \vec{\psi}_I(\vec{r}) \times \vec{r}, & \vec{\Psi}(\vec{r}) &\stackrel{def}{=} \langle \vec{r} | \vec{\Psi} \rangle, \\ \vec{\Psi}(\vec{g}) &\equiv \vec{\psi}_C(\vec{g}) \times \vec{\psi}_J(\vec{g}) \times \vec{\psi}_I(\vec{g}) \times \vec{g}, & \vec{\Psi}(\vec{g}) &\stackrel{def}{=} \langle \vec{g} | \vec{\Psi} \rangle, \\ \vec{\Psi}(\vec{b}) &\equiv \vec{\psi}_C(\vec{b}) \times \vec{\psi}_J(\vec{b}) \times \vec{\psi}_I(\vec{b}) \times \vec{b}, & \vec{\Psi}(\vec{b}) &\stackrel{def}{=} \langle \vec{b} | \vec{\Psi} \rangle;\end{aligned}\tag{78}$$

for a depiction of the three distinct  $q\bar{q}$  pairs that are confined to  $T$  along the six-coloring kagome lattice manifold (see Figure 3 in [32]). Therefore, the six-coloring antisymmetric wavefunction components of eqs. (40–42) in [32] become

$$\vec{\Psi}(\vec{r}, \vec{r}) = -\vec{\Psi}(\vec{r}, \vec{r})\tag{79}$$

$$\vec{\Psi}(\vec{g}, \vec{g}) = -\vec{\Psi}(\vec{g}, \vec{g})\tag{80}$$

$$\vec{\Psi}(\vec{b}, \vec{b}) = -\vec{\Psi}(\vec{b}, \vec{b})\tag{81}$$

for the confined quark and antiquark (two-particle) cases in 3D-PPSS and 3D-OPSS.

Next, using eqs. (75–81), the antisymmetric matrix of eq. (43) in [32] is upgraded to

$$\begin{pmatrix} 0 & \vec{\Psi}_{total}(\vec{r}, \vec{g}, \vec{b}) \\ \vec{\Psi}_{total}(\vec{r}, \vec{g}, \vec{b}) & 0 \end{pmatrix},\tag{82}$$

where the expanded 3D antisymmetric wavefunction matrix of eq. (44) in [32] becomes

$$\begin{pmatrix} 0 & \vec{\Psi}(\vec{r}) & \vec{\Psi}(\vec{g}) \\ \vec{\Psi}(\vec{r}) & 0 & \vec{\Psi}(\vec{b}) \\ \vec{\Psi}(\vec{g}) & \vec{\Psi}(\vec{b}) & 0 \end{pmatrix}\tag{83}$$

for  $T$  in 3D-PPSS and 3D-OPSS.

Finally, the CPT-theorem implementation of [32] is revised, which is a fundamental property of  $T$  in eq. (40). The 2D-OPS charge-conjugation of eq. (47) in [32] is upgraded to the 3D-OPS version

$$\delta_C : \begin{cases} \vec{\psi}_{charge}(\vec{t}) & \mapsto -\vec{\psi}_{charge}(\vec{t}) \\ \begin{pmatrix} \vec{\psi}_{charge}(\vec{t})_{\mathbb{R}} \\ \vec{\psi}_{charge}(\vec{t})_{\mathbb{I}} \\ \vec{\psi}_{charge}(\vec{t})_Z \end{pmatrix} & \mapsto \begin{pmatrix} -\vec{\psi}_{charge}(\vec{t})_{\mathbb{R}} \\ -\vec{\psi}_{charge}(\vec{t})_{\mathbb{I}} \\ -\vec{\psi}_{charge}(\vec{t})_Z \end{pmatrix} \\ \begin{pmatrix} |\vec{\psi}_{charge}(\vec{t})| \\ \langle \vec{\psi}_{charge}(\vec{t}) \rangle \\ [\vec{\psi}_{charge}(\vec{t})] \end{pmatrix} & \mapsto \begin{pmatrix} |\vec{\psi}_{charge}(\vec{t})| \\ \langle \vec{\psi}_{charge}(\vec{t}) \rangle \pm \pi \\ [\vec{\psi}_{charge}(\vec{t})] \pm \pi \end{pmatrix}, \end{cases}\tag{84}$$

where in this case the 3D-OPS  $\vec{\psi}_{charge}$  encodes a generic charge state, the parity-transformation of eq. (48) in [32] is upgraded to the 3D-PPS version

$$\delta_P : \begin{cases} \begin{pmatrix} \vec{y}_R \\ \vec{y}_I \\ \vec{y}_Z \end{pmatrix} & \mapsto \begin{pmatrix} -\vec{y}_R \\ -\vec{y}_I \\ -\vec{y}_Z \end{pmatrix} \\ \begin{pmatrix} |\vec{y}| \\ \langle \vec{y} \rangle \\ [\vec{y}] \end{pmatrix} & \mapsto \begin{pmatrix} |\vec{y}| \\ \langle \vec{y} \rangle \pm \pi \\ [\vec{y}] \pm \pi \end{pmatrix} \end{cases}, \quad (85)$$

where  $[\vec{y}] = \frac{M}{|\vec{y}|}$ , and the time-reversal of eq. (49) in [32] is upgraded to the 3D-PPS version

$$\delta_T : \begin{cases} \vec{t} & \mapsto -\vec{t} \\ \begin{pmatrix} \vec{t}_R \\ \vec{t}_I \\ \vec{t}_Z \end{pmatrix} & \mapsto \begin{pmatrix} -\vec{t}_R \\ -\vec{t}_I \\ -\vec{t}_Z \end{pmatrix} \\ \begin{pmatrix} |\vec{t}| \\ \langle \vec{t} \rangle \\ [\vec{t}] \end{pmatrix} & \mapsto \begin{pmatrix} |\vec{t}| \\ \langle \vec{t} \rangle \pm \pi \\ [\vec{t}] \pm \pi \end{pmatrix} \end{cases}, \quad (86)$$

that together comprise a CPT-transformation.

Note that our triplex framework upgrades the “superfluid-Mott insulator transition” for the spontaneous symmetry breaking of [32, 50] from 2D-OPS to 3D-OPS—this leads to the emergence of *three* types of fundamental excitations in  $Y$ :

1. *massless-phase Nambu-Goldstone modes*,
2. *massless-inclination Nambu-Goldstone modes*, and
3. *massive-amplitude “Higgs-like” modes*.

At this point, we’ve provided an introductory example on how the triplex framework of Section 3 can be applied to upgrade the fractional quantum number order parameters of the baryon wavefunction and antisymmetric tensor in [32] from 2D-OPSs to 3D-OPSs.

### 4.3 Quasi-normal modes for Schwarzschild black holes

Here, the complex and triplex framework of Sections 2 and 3 is applied to the (thermal) SBH quasi-normal modes in [39, 40, 41, 42, 43, 44].

Quasi-normal modes are typically labeled as  $\omega_{nl}$ , where  $l$  is the angular momentum quantum number [39, 40, 41, 42, 43, 44]. For each  $l$  ( $l \geq 2$  for gravitational perturbations), there exists a second quantum number, namely the “overtone” one  $n$  ( $n = 1, 2, \dots$ ), which labels the countable sequence of quasi-normal modes [39, 40, 41, 42, 43, 44]. Thus, for

large  $n$  the quasi-normal modes of the SBH become independent of  $l$  and have the following structure [39, 40, 41, 42, 43, 44]

$$\begin{aligned}\omega_n &= \ln 3 \times T_H + 2\pi i(n + \frac{1}{2}) \times T_H + \mathcal{O}(n^{-\frac{1}{2}}) \\ &= \frac{\ln 3}{8\pi M} + \frac{2\pi i}{8\pi M}(n + \frac{1}{2}) + \mathcal{O}(n^{-\frac{1}{2}})\end{aligned}\tag{87}$$

for a strictly thermal approximation, where  $T_H = \frac{1}{8\pi M}$  is the Hawking temperature for a SBH of mass  $M$ .

Immediately we see that eq. (87) contains a *real* term, namely  $\ln 3 \times T_H = \frac{\ln 3}{8\pi M}$ , and an *imaginary* term, namely  $2\pi i(n + \frac{1}{2}) \times T_H = \frac{2\pi i}{8\pi M}(n + \frac{1}{2})$ . Therefore, we can start by first applying the complex framework of Section 2 to encode the 2D feature states of eq. (87). Thus, if the SBH is centered at the 2D-PPS  $\vec{x} \in X$  in dual 3D space-time with the amplitude-radius (or amplitude-modulus)  $R_{horizon} = \epsilon = 2M$ , then we use eq. (23) to define the new *quasi-normal mode 2D-OPS*

$$\begin{aligned}\vec{\psi}_{\omega_n}(\vec{x}) &\equiv \vec{\psi}_{\omega_n}(\vec{x})_{\mathbb{R}} + \vec{\psi}_{\omega_n}(\vec{x})_{\mathbb{I}} \\ &\equiv (\vec{\psi}_{\omega_n}(\vec{x})) = (|\vec{\psi}_{\omega_n}(\vec{x})|, \langle \vec{\psi}_{\omega_n}(\vec{x}) \rangle) = (\vec{\psi}_{\omega_n}(\vec{x})_{\mathbb{R}} + \vec{\psi}_{\omega_n}(\vec{x})_{\mathbb{I}}),\end{aligned}\tag{88}$$

that satisfies the synchronizing Pythagorean and trigonometric interconnection constraints of eq. (22) to establish

$$\begin{aligned}|\vec{\psi}_{\omega_n}(\vec{x})| &\equiv \sqrt{\vec{\psi}_{\omega_n}^2(\vec{x})_{\mathbb{R}} + \vec{\psi}_{\omega_n}^2(\vec{x})_{\mathbb{I}}} = (\omega_0)_n \\ \vec{\psi}_{\omega_n}(\vec{x})_{\mathbb{R}} &\equiv |\vec{\psi}_{\omega_n}(\vec{x})| \cos \langle \vec{\psi}_{\omega_n}(\vec{x}) \rangle = \ln 3 \times T_H = \frac{\ln 3}{8\pi M} \\ \vec{\psi}_{\omega_n}(\vec{x})_{\mathbb{I}} &\equiv |\vec{\psi}_{\omega_n}(\vec{x})| \sin \langle \vec{\psi}_{\omega_n}(\vec{x}) \rangle = 2\pi i(n + \frac{1}{2}) \times T_H = \frac{2\pi i}{8\pi M}(n + \frac{1}{2}),\end{aligned}\tag{89}$$

where the  $(\omega_0)_n$  term is applied in [42, 43, 44].

Moreover, we also recognize that eq. (87) comprises a tertiary term, namely  $\mathcal{O}(n^{-\frac{1}{2}})$ . Therefore, we can subsequently apply the triplex framework of Section 3 to encode the 3D feature states of eq. (87). Thus, if the SBH is located at the 3D-PPS  $\vec{y} \in Y$  in dual 4D space-time, such that eq. (30) illustrates the interconnection of  $X \subset Y$ , then we use eq. (50) to define the new *quasi-normal mode 3D-OPS*

$$\begin{aligned}\vec{\psi}_{\omega_n}(\vec{y}) &\equiv \vec{\psi}_{\omega_n}(\vec{y})_{\mathbb{R}} + \vec{\psi}_{\omega_n}(\vec{y})_{\mathbb{I}} + \vec{\psi}_{\omega_n}(\vec{y})_Z \\ &\equiv (\vec{\psi}_{\omega_n}(\vec{y})) = (|\vec{\psi}_{\omega_n}(\vec{y})|, \langle \vec{\psi}_{\omega_n}(\vec{y}) \rangle, [\vec{\psi}_{\omega_n}(\vec{y})]) = (\vec{\psi}_{\omega_n}(\vec{y})_{\mathbb{R}} + \vec{\psi}_{\omega_n}(\vec{y})_{\mathbb{I}} + \vec{\psi}_{\omega_n}(\vec{y})_Z),\end{aligned}\tag{90}$$

with the 3D-OPS Cartesian components

$$\begin{aligned}
 \vec{\psi}_{\omega_n}(\vec{y})_{\mathbb{R}} &\equiv \ln 3 \times T_H &= \frac{\ln 3}{8\pi M} \\
 \vec{\psi}_{\omega_n}(\vec{y})_{\mathbb{I}} &\equiv 2\pi i(n + \frac{1}{2}) \times T_H &= \frac{2\pi i}{8\pi M}(n + \frac{1}{2}) \\
 \vec{\psi}_{\omega_n}(\vec{y})_Z &\equiv \mathcal{O}(n^{-\frac{1}{2}})
 \end{aligned} \tag{91}$$

from eq. (87), that satisfy the synchronizing Pythagorean and trigonometric interconnection constraints of eq. (49) to establish

$$\begin{aligned}
 |\vec{\psi}_{\omega_n}(\vec{y})| &\equiv \sqrt{\vec{\psi}_{\omega_n}^2(\vec{y})_{\mathbb{R}} + \vec{\psi}_{\omega_n}^2(\vec{y})_{\mathbb{I}} + \vec{\psi}_{\omega_n}^2(\vec{y})_Z} \\
 \langle \vec{\psi}_{\omega_n}(\vec{y}) \rangle &\equiv \arctan\left(\frac{\vec{\psi}_{\omega_n}(\vec{y})_{\mathbb{I}}}{\vec{\psi}_{\omega_n}(\vec{y})_{\mathbb{R}}}\right) \\
 [\vec{\psi}_{\omega_n}(\vec{y})] &\equiv \arccos\left(\frac{\vec{\psi}_{\omega_n}(\vec{y})_Z}{|\vec{\psi}_{\omega_n}(\vec{y})|}\right).
 \end{aligned} \tag{92}$$

At this point, we've provided an introductory example on how the triplex framework of Section 3 can be applied to encode the SBH quasi-normal modes of [39, 40, 42, 43, 44].

## 5 Conclusion and discussion

In this paper, we started by considering the importance of the complex numbers and spherical structures. It is known that complex numbers are fundamental to science and engineering because their representational capability supercedes that of real numbers [2, 3]. Additionally, spherical structures and spherically-symmetric frameworks (including circles and circularly-symmetric frameworks) are also axiomatic in this context because physical objects and patterns that are observed nature (i.e. baryons, stars, black holes, etc.) frequently exhibit spherical-like properties in a 3D space that can be inferred from the Inopin Holographic Ring of [32] due to the holographic principle [10, 11, 12]. These notions fueled our motivation to explore such spherical relationships in chaotic systems and thereby extend the complex numbers to introduce and define triplex numbers that are consistent with the work of D. White and P. Nylander [33, 34, 35].

The fact that complex and triplex numbers can be simultaneously interpreted and implemented as abstract scalars and vectors was a powerful realization in terms of general applicability to particle and astro physics. From this, it became clear that these constructs could be utilized to define state spaces for locations in space-time and features at such locations. Thus, our next step was to employ the complex numbers to establish the well-defined 2D-PPS, 2D-PPSS, 2D-OPS, and 2D-OPSS information structures to improve the topology and simultaneous and spontaneous superfluidic symmetry breaking of [32]. Subsequently, we repeated a similar creative upgrade to [32] with the additional spatial dimension, where we engaged the triplex numbers to assemble definitions for the 3D-PPS, 3D-PPSS,

3D-OPS, and 3D-OPSS information structures. Afterwards, we provided three distinct and preliminary examples on how these new information structures can be applied to encode the White-Nylander mythical beast of [33, 34, 35], the baryon-antibaryon wavefunction of [32], and the SBH quasi-normal modes of [39, 40, 41, 42, 43, 44]. Thus, the encoding formulations of this complex and triplex framework are highly consistent and disciplined, and thereby provide an easy-to-visualize, relatively simplistic, and flexible system of abstract vectors—attributes that are, in our opinion, important from an engineering and applicability standpoint. Moreover, we suggest that such an encoding methodology and framework with built-in (spherically-symmetric) non-linearity that complies with three spatial dimensions and a fourth temporal dimension, where space and time are dual and interconnected, is crucial for attacking problems and representing chaotic system states in physics and computer science.

For future work, we propose that the content of this paper should undergo additional consideration, scrutiny, and clarification. In particular, it may be beneficial and enlightening to apply the complex and triplex framework of this paper to further analyze the baryon wavefunction and antisymmetric tensors of [32], along with the tensors of general relativity [51] and the Brans-Dicke theory of gravitation [52]. Furthermore, computer simulations should be conducted to generate 3D fractals and the Mandelbulb [33, 34, 35] in this latest version of the Riemannian dual space-time topology.

## 6 Acknowledgement

I wish to thank the anonymous referees for the constructive criticisms and comments that enhanced the quality and application of this paper. In particular, one referee enlightened me with praiseworthy insight on triplex fractals. Also, I wish to thank A. E. Inopin for guiding me through the raging frontiers of physics during our relentless storm of quark confinement [32]—the framework of this paper is principally inspired by our insistent questioning, arguments, and collaboration.

## References

- [1] L. Floridi. *Information: A very short introduction*. OUP Oxford, 2010.
- [2] C. P. McKeague. *Elementary algebra*. Brooks/Cole Publishing Company, 2011.
- [3] D. Alpay. Complex numbers: Algebra. In *A Complex Analysis Problem Book*, pages 11–60. Springer, 2011.
- [4] T. P. Cheng and L. F. Li. *Gauge theory of elementary particle physics*. Clarendon Press Oxford, 1984.
- [5] J. Vlach. *Computer methods for circuit analysis and design*. Springer, 1983.
- [6] H. O. Peitgen, H. Jürgens, and D. Saupe. *Chaos and fractals: new frontiers of science*. Springer, 2004.
- [7] B. B. Mandelbrot. *The fractal geometry of nature*. Times Books, 1982.
- [8] R. F. Voss. *Fractals in nature: characterization, measurement, and simulation*. IBM Thomas J. Watson Research Center, 1987.

- [9] G. W. Flake. *The computational beauty of nature: Computer explorations of fractals, chaos, complex systems and adaption*. The MIT Press, 1998.
- [10] L. Susskind. The world as a hologram. *arXiv preprint hep-th/9409089*, 1994.
- [11] R. Bousso. The holographic principle. *Rev. Mod. Phys.*, 74:825–874, Aug 2002.
- [12] G. 't Hooft. Dimensional reduction in quantum gravity. *arXiv preprint arXiv:gr-qc/9310026*, 2009.
- [13] C. W. Misner and D. H. Sharp. Relativistic equations for adiabatic, spherically symmetric gravitational collapse. *Physical Review*, 136(2B):B571, 1964.
- [14] H. P. Künzle and A. K. M. Masood-ul Alam. Spherically symmetric static SU (2) Einstein–Yang–Mills fields. *Journal of Mathematical Physics*, 31(4):928–935, 1990.
- [15] H. P. Künzle. Analysis of the static spherically symmetric SU (N) Einstein–Yang–Mills equations. *Communications in mathematical physics*, 162(2):371–397, 1994.
- [16] H. A. Kastrup and T. Thiemann. Spherically symmetric gravity as a completely integrable system. *Nuclear Physics B*, 425(3):665–686, 1994.
- [17] K. Martel and E. Poisson. Regular coordinate systems for Schwarzschild and other spherical spacetimes. *arXiv preprint gr-qc/0001069*, 2000.
- [18] T. Dray and G. 't Hooft. The effect of spherical shells of matter on the Schwarzschild black hole. *Communications in Mathematical Physics*, 99(4):613–625, 1985.
- [19] A. Nagar and L. Rezzolla. Gauge-invariant non-spherical metric perturbations of Schwarzschild black-hole spacetimes. *Classical and Quantum Gravity*, 22(16):R167, 2005.
- [20] P. H. Hauschildt, F. Allard, Ferguson, E. J., Baron, and D. R. Alexander. The NEXTGEN model atmosphere grid. II. spherically symmetric model atmospheres for giant stars with effective temperatures between 3000 and 6800 K. *The Astrophysical Journal*, 525(2):871, 2009.
- [21] M. Rampp and J. T. Janka. Spherically symmetric simulation with Boltzmann neutrino transport of core collapse and postbounce evolution of a 15  $M_{\odot}$  star. *The Astrophysical Journal Letters*, 539(1):L33, 2008.
- [22] F. Allard, P. H. Hauschildt, and A. Schweitzer. Spherically symmetric model atmospheres for low-mass pre-main-sequence stars with effective temperatures between 2000 and 6800 K. *The Astrophysical Journal*, 539(1):366, 2008.
- [23] V. M. Strutinsky. Shell effects in nuclear masses and deformation energies. *Nuclear Physics A*, 95(2):420–442, 1967.
- [24] I. Klebanov. Nuclear matter in the Skyrme model. *Nuclear Physics B*, 262(1):133–143, 1985.
- [25] T. Ioannidou, B. Piette, and W. J. Zakrzewski. Spherically symmetric solutions of the SU (N) Skyrme models. *arXiv preprint hep-th/9904160*, 1999.
- [26] N. D. Mermin. The topological theory of defects in ordered media. *Reviews of Modern Physics*, 51(3):591, 1979.
- [27] H. Toyoki. Structure factors of vector-order-parameter systems containing random topological defects. *Physical Review B*, 45(5):1965, 1992.
- [28] J. Montagnat, H. Delingette, and N. Ayache. A review of deformable surfaces: topology,

- geometry and deformation. *Image and vision computing*, 19(14):1023–1040, 2001.
- [29] Q. Du, C. Liu, and X. Wang. Simulating the deformation of vesicle membranes under elastic bending energy in three dimensions. *Journal of Computational Physics*, 212(2):757–777, 2006.
- [30] T. Liko. Topological deformation of isolated horizons. *Physical Review D*, 77(6):064004, 2008.
- [31] P. Coullet, C. Elphick, L. Gil, and J. Lega. Topological defects of wave patterns. *Physical review letters*, 59(8):884–887, 1987.
- [32] A. E. Inopin and N. O. Schmidt. Proof of quark confinement and baryon-antibaryon duality: I: Gauge symmetry breaking in dual 4D fractional quantum Hall superfluidic space-time. *Hadronic Journal*, 35(5):469–506, 2012.
- [33] P. Nylander. Hypercomplex fractals, 2009.
- [34] D. White. The mystery of the real, 3D Mandelbrot fractal, 2009.
- [35] T. Boniecki. Soler 7 - using rotational matrices to generate triplex algebras, 2010.
- [36] E. N. Lorenz. Deterministic nonperiodic flow. *Journal of the atmospheric sciences*, 20(2):130–141, 1963.
- [37] S. H. Kellert. *In the wake of chaos: Unpredictable order in dynamical systems*. University of Chicago Press, 1993.
- [38] K. Nomizu and K. Yano. On circles and spheres in Riemannian geometry. *Mathematische Annalen*, 210(2):163–170, 1974.
- [39] S. Hod. Bohr’s correspondence principle and the area spectrum of quantum black holes. *Physical Review Letters*, 81:4293, 1998.
- [40] S. Hod. Gravitation, the quantum, and Bohr’s correspondence principle. *General Relativity Gravity*, 31:1639, 1999.
- [41] M. Maggiore. Physical interpretation of the spectrum of black hole quasinormal modes. *Physical Review Letters*, 100:141301, 2008.
- [42] C. Corda. Effective temperature for black holes. *Journal of High Energy Physics*, 1108:101, 2011.
- [43] C. Corda. Effective temperature, Hawking radiation and quasinormal modes. *International Journal of Modern Physics D*, 21:1242023, 2012.
- [44] C. Corda. Black hole’s quantum levels. *arXiv:1210.7747*, 2012.
- [45] J. Friedman, M. S. Morris, I. D. Novikov, and F. Echeverria. Cauchy problem in spacetimes with closed timelike curves. *Physical Review D*, 42(6):1915, 1990.
- [46] G. Springer. *Introduction to Riemann surfaces*. Chelsea Publishing Company, 1981.
- [47] C. F. Diether III and A. E. Inopin. Quantum vacuum charge and the new hypercp particle x. *arXiv preprint physics/0601110*, 2006.
- [48] J. Rampe. *Softology - Visions of Chaos*, 2013.
- [49] V. Mourik, K. Zuo, S. M. Frolov, and S. R. Plissard. Signatures of Majorana fermions in hybrid superconductor-semiconductor nanowire devices. *Arxiv preprint arXiv:1204.2792*, 2012.
- [50] M. Endres, T. Fukuhara, D. Pekker, M. Cheneau, P. Schauß, C. Gross, E. Demler, S. Kuhr, and I. Bloch. The ‘Higgs’ amplitude mode at the two-dimensional super-

- fluid/Mott insulator transition. *Nature*, 487(7408):454–458, 2012.
- [51] C. W. Misner, K. S. Thorne, and J. A. Wheeler. *Gravitation*. WH Freeman, 1973.
- [52] C. Brans and R. H. Dicke. Mach’s principle and a relativistic theory of gravitation. *Physical Review*, 124:925–935, 1961.